厚生労働科学研究費補助金

難病・がん等の疾患分野の医療の実用化研究事業

（再生医療関係研究分野）

有害事象発生時の科学的な細胞検証を通じて細胞治療の安全性向上を目指す

臨床用細胞保管・検査拠点の構築

平成25年度　総括・分担研究報告書

公財）先端医療振興財団　細胞療法開発事業部門

研究代表者　川真田　伸

目　次

はじめに

本報告書は、厚生労働科学研究費補助金　難病・がん等の疾患分野の医療の実用化研究事業の再生医療関係研究分野の一つである「有害事象発生時の科学的な細胞検証を通じて細胞治療の安全性向上を目指す臨床用細胞保管・検査拠点の構築」研究班における平成25年度の研究成果をまとめたものである。

平成24年度にiPS細胞等の臨床研究安全基盤整備事業として、iPS細胞等を活用した細胞移植治療におけるヒト幹細胞アーカイブとが整備された。本研究は、移植に用いたヒト幹細胞の一部を「ヒト幹細胞アーカイブ」に保管しておき、移植から時間が経過した後に、移植に用いたヒト幹細胞について溯って調べることを可能にしておくことで、ヒト幹細胞移植の安全性・有効性を長期的にフォローアップでき、安全かつ有効な再生医療を実現、臨床研究が促進されることにつながる事を目的としている。本目的を達成するために、平成25年度では下記のテーマの分担研究を行い、「有害事象発生時の科学的な細胞検証を通じて細胞治療の安全性向上を目指す臨床用細胞保管・検査拠点の構築」に関する研究を実施した。

1．　移殖検体の保管

2．　移殖検体の細胞評価研究

3．　臨床的意義を示すための細胞検査の実施

4．　保管業務支援として事務局の設置

上記のテーマ別研究課題について、平成 25 年度時点　中間報告書（1 年目）として作成したものであるが、関係者のご参考になれば幸いである。

また、iPS 細胞を活用し臨床研究の実施を計画されている諸先生方の治療法が、より安全で国内外へ広く発展するための事業として、ヒト幹細胞アーカイブが成熟できるよう強く期待している。

平成25年度厚生科研研究「有害事象発生時の科学的な細胞検証を通じて細胞治療の安全性向上を目指す臨床用細胞保管・検査拠点の構築」研究班

研究組織

	役　割	氏　名	所　属
研究代表者	研究総括	川真田　伸	公財）先端医療振興財団　細胞療法開発事業部門
分担研究者	細胞検査 責任者	郷　正博	公財）先端医療振興財団　細胞療法開発事業部門 細胞製造グループ
分担研究者	細胞保管/細胞評価研究責任者 (兼)細胞保管事務局長	西下　直希	公財）先端医療振興財団　細胞療法開発事業部門 細胞評価グループ
協力研究者		永田　洋二	臨床研究情報センター
協力研究者		川本　篤彦	先端医療センター病院　診療部　再生治療ユニット
協力研究者		橋本　尚子	先端医療センター病院　細胞管理センター
協力研究者		田口　明彦	先端医療センター研究所　再生医療研究部
協力研究者		高橋　政代	理化学研究所　発生・再生科学総合研究センター
協力研究者		金村　星余	公財）先端医療振興財団　細胞療法開発事業部門　細胞評価グループ
協力研究者		鹿村　真之	公財）先端医療振興財団　細胞療法開発事業部門　細胞評価グループ
協力研究者		村松　万里江	公財）先端医療振興財団　細胞療法開発事業部門　細胞評価グループ
協力研究者		山本　貴子	公財）先端医療振興財団　細胞療法開発事業部門　細胞評価グループ
協力研究者		竹中　ちえみ	公財）先端医療振興財団　細胞療法開発事業部門　細胞評価グループ
	細胞保管事務局	清水　良雄	公財）先端医療振興財団　細胞療法開発事業推進課
	細胞保管事務局	林　直哉	公財）先端医療振興財団　細胞療法開発事業推進課
	細胞保管事務局	竹内　勝信	公財）先端医療振興財団　細胞療法開発事業推進課
	細胞保管事務局	ジェイコブスいずみ	公財）先端医療振興財団　細胞療法開発事業推進課

厚生労働科学研究費補助金（研究事業）

総括研究報告書

有害事象発生時の科学的な細胞検証を通じて細胞治療の安全性向上を目指す臨床用細胞保管・検査拠点の構築

研究代表者：川真田　伸

（公財）先端医療振興財団　細胞療法開発事業部門　副事業統括

研究要旨

再生医療を普及させる上で重要な社会基盤の一つとして、「細胞移殖治療の安全性、信頼性を担保する基盤構築」が挙げられる。移植に用いたヒト幹細胞の一部を「ヒト幹細胞アーカイブ」に保管しておき、移植から時間が経過した後に、移植に用いたヒト幹細胞について溯って調べることを可能にしておくことで、細胞移植の安全性・有効性を長期的にフォローアップでき、安全かつ有効な再生医療を実現できる。このような安全・安心な細胞治療の普及を目指す社会基盤構築として、先端医療振興財団ではヒト幹細胞アーカイブを活用し、将来的に細胞治療の安全性が損なわれないように、移殖細胞の保管と情報管理および移植後の治療効果検証による再生医療産業化プラットフォーム作りを目指す。

本事業では上記の社会実現のために、1．移殖検体の保管 2．移殖検体の細胞評価研究　3．臨床的意義を示すための細胞検査の実施，細胞検査技術の開発/細胞標準化・規格化　4.細胞保管業務に関する運営管理基準および細胞寄託に対する事務業務を統合的に構築する必要がある。

本年度の成果としては、細胞療法開発事業部門内にて細胞保管業務と細胞検査業務部隊を構築し、ヒト幹細胞アーカイブ用 HP の立ち上げ、細胞保管事務局を設置、保管寄託業務に対する運用基準を構築した。その他、細胞評価研究についても、オミックス解析を活用した細胞評価技術の構築を行った。また、細胞検査技術では、染色体解析業務を自施設で実施可能とし、M-FISH や M-BAND 等の検査体制を構築した。

【研究目的】

再生医療の普及は日本成長戦略の重要課題の一つであり、今年にはiPS細胞由来網膜色素上皮細胞を用いた加齢黄斑変性治療の臨床研究実施が予定されている。再生医療を普及させる上で、iPS細胞に関する分化誘導技術や細胞検査技術のような基礎医学的な研究技術、移殖細胞に対する品質の安全性データ構築等に加えて、移植細胞の情報管理および移植後の治療効果検証による「細胞移殖治療の安全性、信頼性を担保する社会基盤の構築」こそ、再生医療産業化における第一歩である。このような社会基盤構築のため、先端医療振興財団ではヒト幹細胞アーカイブを活用し、将来的に細胞治療の安全性が損なわれないような体制構築を目指している。

【研究方法】

本事業では、臨床研究実施機関に加え、第三者機関として移植細胞の保管・細胞検査を集約的に実施し、検査手法・結果判定の規格化と検査内容公開による情報共有の仕組を作ることで、安全性向上に貢献することを課題としている。（図1）

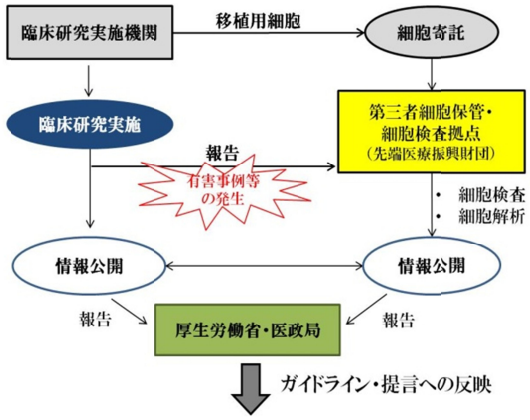

図１．有害害事象発生時の科学的な細胞検証をする細胞の保管、検査拠点の役割

事業実施にあたり当該年度では機関内で組織編成。保存検体の種類・管理方法・運用規定等を構築した。

【研究結果】

細胞療法開発事業部門内にて細胞保管業務と細胞検査業務部隊を構築し、細胞保管研究/細胞評価研究/細胞保管・管理業務と細胞検査の実施/細胞検査技術の開発/細胞標準化・規格化とに役割を分担した。加えて、細胞保管に対する契約/細胞情報保管/ホームページの運営管理等の業務を細胞保管業務内に事務局を設置し、保管業務に対する事務業務を支援する体制も同時に整えた。（図2）

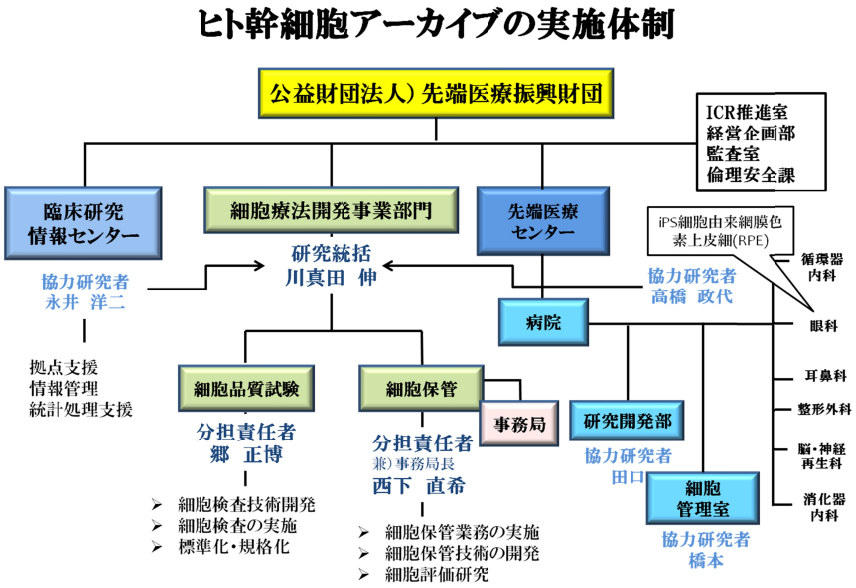

図2. 公益財団法人）先端医療振興財団のヒト幹細胞アーカイブ実施体制図

また、万一の有害事例発生時に細胞検証するために必要な細胞保管体制として、iPS細胞由来網膜色素上皮細胞（加齢黄斑変性治療）の場合、Fibroblast細胞（細胞源:①）、Fibroblast細胞から樹立したiPS細胞（樹立iPS細胞:②）、iPS細胞から分化させたRPE細胞（iPS由来RPE細胞:③）、RPE細胞のマウス皮下移殖試験後の組織細胞）造腫瘍性実施細胞:④）、移殖使用したRPE細胞（最終分化細胞:⑤）の各ステップの細胞を保管する事を確定した。（図3）

【考察】

本事業は、幹細胞治療に使われた細胞の保管事業だけでなく、有害事象発生時の検査を第三者機関として実施することで、細胞治療の安全性向上に大いに寄与すると考える。

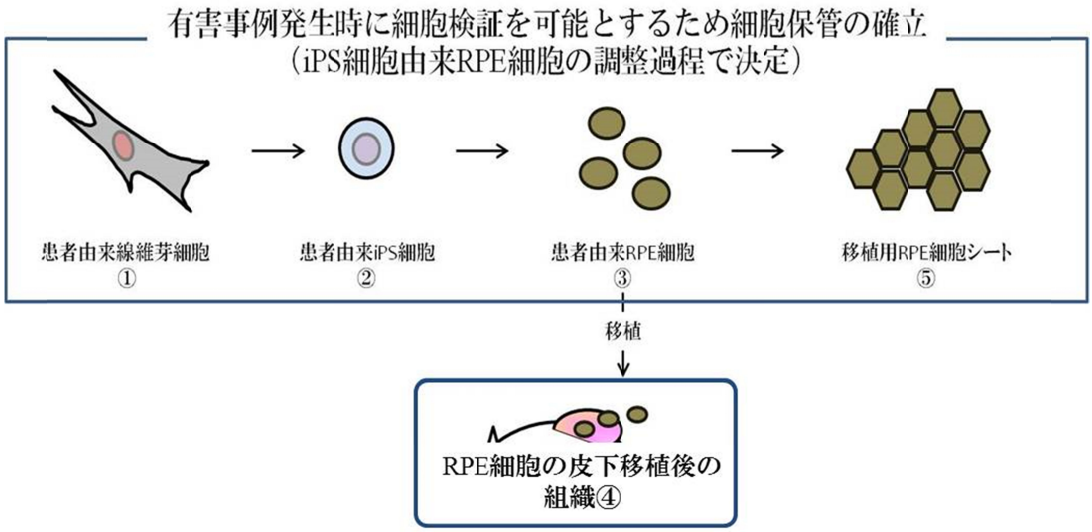

図3. 先端医療振興財団のヒト幹細胞アーカイブで細胞検証を可能とするための、検体保管体制

厚生労働科学研究費補助金（研究事業）

分担研究報告書

細胞検査のための染色体解析技術の確立

分担研究者:郷　正博

（公財）先端医療振興財団　細胞療法開発事業部門　細胞製造グループ

研究要旨

万一の有害事例発生時に細胞検証する際に、正しい細胞評価が行わなければ、原因探索や再発防止を考察するに十分な科学的結果が反映できず、細胞移植治療に対する安全性の検証ができない。臨床的知見を基に、細胞調整段階、あるいは移殖直前の細胞を検証することも原因探索研究を行う上で、非常に重要である。

本研究では、細胞培養時、調整時に起きやすいとされる染色体異常(Hotspot)と臨床的有害事例を組み合わせた検査を実施するため、当該年度では染色体解析技術(M-FISH 法、M-BAND 法)を立ち上げ、染色体解析に対する早期解析評価できる技術を確立した。

【研究目的】

細胞の安全性評価については、細胞調整段階、移殖直前、凍結前後の細胞の染色体解析が不可欠であり形態学的な染色体評価手技（G-band法，M-FISH，M-BAND技術）での検証は重要課題の一つである。当該年度では、染色体異常の検証を素早く実施可能とするため、染色体解析技術(M-FISH法、M-BAND法)を立ち上げ、染色体解析に対する早期解析評価できる技術を確立した。

【研究方法】

細胞検査技術開発として、当該年度ではG-band法に加え、M-FISH法、M-BAND法の解析を実施した。細胞は、ES細胞(khES-1株)を用いて評価した。

【結果】

M-FISH解析の結果、各クロモゾーム別の染色が確認でき、正常細胞株である事がわかった。（図6）また、m-BAND解析を実施し、khES-1細胞のChr.1領域は、正常であることを確認した。

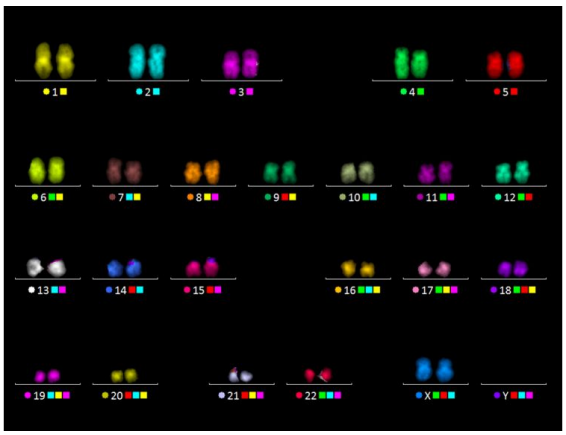

図 6.　M-FISH 解析　(khES-1 細胞株)

【考察】

当該年度では、形態学的な構造異常を検証できる染色体技術を確立した。次年度より、CGH array等のマイクロアレイ技術を用いた染色体解析技術を導入し、細胞凍結や継代培養におけるgene stabilityや造腫瘍性に関する検査法の開発を着手する予定である。

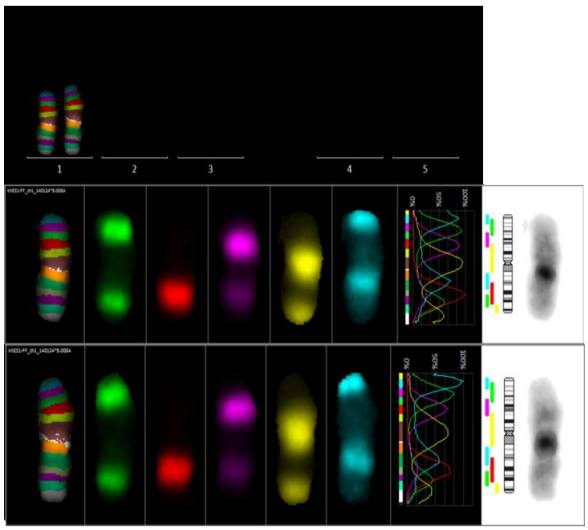

図7.　khES-1細胞株のchr.1 のM-BAND

厚生労働科学研究費補助金（研究事業）

分担研究報告書

移植後の保存検体(細胞・組織)からの細胞評価法の開発および ヒト幹細胞アーカイブ運用における細胞保管管理の体制の確立

分担研究者：西下　直希

（公財）先端医療振興財団　細胞療法開発事業部門　細胞評価グループ

研究要旨

有害事例発生時に細胞検証する際に、正しい細胞評価より原因探索を行い、科学的結果を反映することが、細胞移植治療に対する安全性の検証となる。このような原因探索を検討するための細胞評価手法を考案するためには、最終産物に近い細胞、移植後の細胞あるいは組織から移植細胞の状況をフィードバックできる評価法を開発する必要がある。この技術開発こそ、細胞移殖治療の安全性、有効性の検証に繋がり、細胞規格化・標準化になるものと考えられる。

当該年度の細胞評価研究課題としては、移植後の細胞・組織で検証可能とする細胞評価方法の確立、原因探索法に対する検討を行う。具体的には、移植細胞に（非腫瘍性）分化中間体の混入があるかを評価するために、皮下移殖試験後の組織から DNA を回収後、メチル化解析情報を得た。結果として、移殖後の組織から最終分化細胞のみを移殖した事例なのか、分化中間体の混入がある事例なのか、移植時の細胞状況をフィードバックできる事が分かった。

また、細胞保管体制の構築として、ヒト幹細胞アーカイブ運用に対する運用規定の作成、細胞寄託促進のために HP の開設、細胞保管手順書の作成、細胞保管/管理システムを構築した。

【研究目的】

万一の有害事例発生時に細胞検証する際に、正しい細胞評価が行わなければ、原因探索や再発防止を考察するに十分な科学的結果が反映できず、細胞移植治療に対する安全性の検証ができない。このような原因探索のための細胞評価手法を考案するためには、最終産物に近い細胞あるいは移植後の細胞・組織から移植時の細胞情報をフィードバックできる評価法を開発する必要がある。当該年度の細胞評価研究では、移植後の細胞検証と原因追究を可能とする評価研究方法として、①メチル化解析, ②オミックス解析 ③代謝解析を実施した。

【研究方法】

移植後の細胞組織から移殖時の細胞情報をフィードバックできる評価法として、皮下移殖試験後の組織から細胞情報を獲得、評価した。具体的には、昨年度のJST「多能性幹細胞由来移植細胞の安全性評価研究」実施時に得た3th RPE移殖組織片（非造腫瘍性分化中間体混入が著明なRPE細胞）と4th RPE移殖組織片（非造腫瘍性分化中間体混入が見られない最終RPE移殖細胞）を提供頂き、上記2種の組織からDNAを抽出し、Illumina Infinium HD Methylation にて比較解析した。

【結果】

Terminal differentiationした4^{th} RPE細胞で非メチル化、3^{th} RPE細胞でメチル化が確認できた領域を抽出した。(Table 1) PFKM, TNFSF8, LFNG, DMD, ETV1などの領域は、ヒトMSC細胞でもメチル化していることを確認し、さらにRPE細胞でメチル化されていると考えられるEpithelial cell transforing sequence 2 oncogene-like (ECT2L) は、3^{th} RPE細胞と4^{th} RPE細胞の両者でメチル化に差が見られなかった。PFKM, TNFSF8, LFNG, DMD, ETV1領域のMethylation評価(不純物混入を評価した手法)は、RPE細胞の移植後の経過観察試験として有効な評価系となる可能性を示唆した。

【考察】

今後、n数を増やして検証する必要性もあると考えている。以上の結果より、移植後の有害事例発生時における細胞検査項目としてMethylation解析は、有用な手段である可能性を示唆した。

Table 1. 非造腫瘍性分化中間体混入 RPE 細胞と最終分化 RPE 細胞とのメチル化の違い

									倍率		範囲内				変動幅		結果
UTR---Index	hMSC	59G 3thRPE	59G 4thRPE	ProbeID	ENTREZ_GENEID	TYPE_OF_GENE	GENE_SYMBOL	DESCRIPTION	59G 3thRPE VS 59G 4thRPE		59G 3thRPE VS hMSC		59G 4thRPE VS hMSC		hMSC,59G 3thRPE,59G 4thRPEの最大値と最小値の幅が指		59G 3thRPEと59G 4thRPEがn倍離れていて,hMSCとm倍以内の個数
									59G 3thRPEがn倍大きい	1.5	二つのデータがm倍以内	1.5	二つのデータがm倍以内	0	指定値以上	10	
									59G 4thRPEがn倍大きい								
									個数	**770**	個数	**12648**	個数	**0**	個数	**8068**	**116**
										判定	比率	判定	比率	判定	幅	判定	判定
206	85.7	67.2	38.0	cg10508111;cg162	5213	protein-coding	PFKM	phosphofructokinase, muscle		O	1.3	O	2.3		47.7	O	O
380	31.1	33.2	8.6	cg14725537	5354	protein-coding	PLP1	proteolipid protein 1		O	1.1	O	3.6		24.6	O	O
522	32.3	31.4	10.7	cg05726661	1140	protein-coding	CHRNB1	cholinergic receptor, nicotinic, beta 1 (muscle)		O	1.0	O	3.0		21.7	O	O
890	67.0	59.6	28.5	cg27631256	944	protein-coding	TNFSF8	tumor necrosis factor (ligand) superfamily, member 8		O	1.1	O	2.3		38.5	O	O
1229	49.3	65.0	20.7	cg15016628	680	protein-coding	BRS3	bombesin-like receptor 3		O	1.3	O	2.4		44.3	O	O
1268	56.1	51.6	20.8	cg12971694	971	protein-coding	CD72	CD72 molecule		O	1.1	O	2.7		35.3	O	O
1542	60.5	82.8	51.3	cg19807685	3294	protein-coding	HSD17B2	hydroxysteroid (17-beta) dehydrogenase 2		O	1.4	O	1.2		31.5	O	O
1650	84.0	81.0	46.5	cg20572537	3955	protein-coding	LFNG	LFNG O-fucosylpeptide 3-beta-N-acetylglucosaminyltransferase		O	1.0	O	1.8		37.5	O	O
1762	53.0	52.8	14.2	cg20171297	4618	protein-coding	MYF6	myogenic factor 6 (herculin)		O	1.0	O	3.7		38.7	O	O
1865	90.5	66.8	30.9	cg26266308	5150	protein-coding	PDE7A	phosphodiesterase 7A		O	1.4	O	2.9		59.6	O	O
2222	77.4	80.3	52.7	cg01634964;cg023	6597	protein-coding	SMARCA4	SWI/SNF related, matrix associated, actin dependent regulator of chromatin, subfamily a, member 4		O	1.0	O	1.5		27.6	O	O
2371	75.7	66.4	42.6	cg08485937	7134	protein-coding	TNNC1	troponin C type 1 (slow)		O	1.1	O	1.8		33.1	O	O
2432	80.9	78.3	50.3	cg02399030;cg070	7378	protein-coding	UPP1	uridine phosphorylase 1		O	1.0	O	1.6		30.7	O	O
2572	69.7	82.5	53.0	cg10533161	8428	protein-coding	STK24	serine/threonine kinase 24		O	1.2	O	1.3		29.5	O	O
2879	57.8	73.1	42.0	cg02629615;cg261	1756	protein-coding	DMD	dystrophin		O	1.3	O	1.4		31.1	O	O
3204	55.6	73.7	46.3	cg00346556;cg019	2059	protein-coding	EPS8	epidermal growth factor receptor pathway substrate 8		O	1.3	O	1.2		27.4	O	O
3546	54.5	65.7	34.5	cg02151632;cg047	9583	protein-coding	ENTPD4	ectonucleoside triphosphate diphosphohydrolase 4		O	1.2	O	1.6		31.2	O	O
3637	55.7	69.4	45.5	cg03512369;cg047	5358	protein-coding	PLS3	plastin 3		O	1.2	O	1.2		23.9	O	O
3817	65.6	74.2	47.0	cg22148297	2841	protein-coding	GPR18	G protein-coupled receptor 18		O	1.1	O	1.4		27.2	O	O
4000	50.7	68.3	43.4	cg04036101;cg040	3801	protein-coding	KIFC3	kinesin family member C3		O	1.3	O	1.2		24.9	O	O
4414	49.0	38.5	25.4	cg21166775	10411	protein-coding	RAPGEF3	Rap guanine nucleotide exchange factor (GEF) 3		O	1.3	O	1.9		23.6	O	O
4905	54.3	39.0	14.1	cg17548735	10930	protein-coding	APOBEC2	apolipoprotein B mRNA editing enzyme, catalytic polypeptide-like 2		O	1.4	O	3.9		40.2	O	O
5020	72.1	62.9	40.1	cg21573263	6536	protein-coding	SLC6A9	solute carrier family 6 (neurotransmitter transporter, glycine), member 9		O	1.1	O	1.8		32.0	O	O
5234	40.2	33.7	11.6	cg23051598	11273	protein-coding	ATXN2L	ataxin 2-like		O	1.2	O	3.5		28.6	O	O
5523	47.3	42.3	27.0	cg02294539;cg219	23548	protein-coding	TTC33	tetratricopeptide repeat domain 33		O	1.1	O	1.8		20.3	O	O
5657	58.7	55.4	29.4	cg02290197;cg066	29887	protein-coding	SNX10	sorting nexin 10		O	1.1	O	2.0		29.2	O	O
6041	44.1	59.0	34.7	cg25447894	27254	protein-coding	CSDC2	cold shock domain containing C2, RNA binding		O	1.3	O	1.3		24.3	O	O
7106	55.9	39.1	25.2	cg03509901	51701	protein-coding	NLK	nemo-like kinase		O	1.4	O	2.2		30.7	O	O
7179	67.9	61.5	40.6	cg02059867;cg027	51195	protein-coding	RAPGEFL1	Rap guanine nucleotide exchange factor (GEF)-like 1		O	1.1	O	1.7		27.3	O	O
8382	27.9	39.7	14.7	cg01003803;cg068	26281	protein-coding	FGF20	fibroblast growth factor 20		O	1.4	O	1.9		24.9	O	O

Table 1(続き).

非造腫瘍性分化中間体混入 RPE 細胞と最終分化 RPE 細胞とのメチル化の違い

8598	83.1	84.5	54.4	cg10565645	2589	protein-coding	GALNT1	UDP-N-acetyl-alpha-D-galactosamine:polypeptide N-acetylgalactosaminyltransferase 1 (GalNAc-T1)		O	1.0	O	1.5		30.1	O	O
8720	74.3	80.1	33.0	cg10576828	57554	protein-coding	LRRC7	leucine rich repeat containing 7		O	1.1	O	2.3		47.1	O	O
9127	57.2	66.7	40.0	cg02458882;cg060	10133	protein-coding	OPTN	optineurin		O	1.2	O	1.4		26.7	O	O
10125	79.9	59.5	34.5	cg02218324;cg179	81492	protein-coding	RSPH6A	radial spoke head 6 homolog A (Chlamydomonas)		O	1.3	O	2.3		45.4	O	O
10624	80.8	86.0	52.5	cg11081809						O	1.1	O	1.5		33.6	O	O
10691	61.4	75.7	40.1	cg02391387;cg027	83943	protein-coding	IMMP2L	IMP2 inner mitochondrial membrane peptidase-like (S. cerevisiae)		O	1.2	O	1.5		35.6	O	O
10722	65.6	62.7	41.1	cg00831247;cg089	84695	protein-coding	LOXL3	lysyl oxidase-like 3		O	1.0	O	1.6		24.6	O	O
10817	69.7	62.6	41.3	cg00677195	80760	protein-coding	ITIH5	inter-alpha-trypsin inhibitor heavy chain family, member 5		O	1.1	O	1.7		28.4	O	O
11157	75.7	70.5	43.4	cg06494770;cg074	90293	protein-coding	KLHL13	kelch-like 13 (Drosophila)		O	1.1	O	1.7		32.3	O	O
11787	80.6	61.4	40.8	cg01513802	23345	protein-coding	SYNE1	spectrin repeat containing, nuclear envelope 1		O	1.3	O	2.0		39.8	O	O
11972	83.1	86.6	54.8	cg04908300;cg161	5468	protein-coding	PPARG	peroxisome proliferator-activated receptor gamma		O	1.0	O	1.5		31.7	O	O
12056	87.0	67.1	44.1	cg02462253;cg182	5602	protein-coding	MAPK10	mitogen-activated protein kinase 10		O	1.3	O	2.0		42.8	O	O
12525	40.2	33.7	11.6	cg23051598	11273	protein-coding	ATXN2L	ataxin 2-like		O	1.2	O	3.5		28.6	O	O
12543	79.6	58.8	23.6	cg00609333;cg045	4257	protein-coding	MGST1	microsomal glutathione S-transferase 1		O	1.4	O	3.4		56.0	O	O
12579	37.9	31.2	17.2	cg01745499;cg026	3159	protein-coding	HMGA1	high mobility group AT-hook 1		O	1.2	O	2.2		20.7	O	O
12580	37.9	31.2	17.2	cg01745499;cg026	3159	protein-coding	HMGA1	high mobility group AT-hook 1		O	1.2	O	2.2		20.7	O	O
12585	37.2	24.8	16.5	cg00561081;cg013	7571	protein-coding	ZNF23	zinc finger protein 23		O	1.5	O	2.2		20.7	O	O
12628	87.0	64.7	43.0	cg11395414	115290	protein-coding	FBXO17	F-box protein 17		O	1.3	O	2.0		44.0	O	O
12636	40.2	33.7	11.6	cg23051598	11273	protein-coding	ATXN2L	ataxin 2-like		O	1.2	O	3.5		28.6	O	O
12637	40.2	33.7	11.6	cg23051598	11273	protein-coding	ATXN2L	ataxin 2-like		O	1.2	O	3.5		28.6	O	O
12638	40.2	33.7	11.6	cg23051598	11273	protein-coding	ATXN2L	ataxin 2-like		O	1.2	O	3.5		28.6	O	O
13154	61.7	54.7	33.5	cg18953104	167838	protein-coding	TXLNB	taxilin beta		O	1.1	O	1.8		28.3	O	O
13406	75.6	60.2	33.3	cg26367031	27094	protein-coding	KCNMB3	potassium large conductance calcium-activated channel, subfamily M beta member 3		O	1.3	O	2.3		42.3	O	O
13705	56.7	48.2	23.1	cg00964137;cg021	285600	protein-coding	KIAA0825	KIAA0825		O	1.2	O	2.5		33.6	O	O
14584	50.3	68.9	38.6	cg00094817;cg004	1390	protein-coding	CREM	cAMP responsive element modulator		O	1.4	O	1.3		30.3	O	O
14587	50.3	68.9	38.6	cg00094817;cg004	1390	protein-coding	CREM	cAMP responsive element modulator		O	1.4	O	1.3		30.3	O	O
14801	48.3	37.9	24.9	cg03508235	84962	protein-coding	AJUBA	ajuba LIM protein		O	1.3	O	1.9		23.4	O	O
14805	42.7	43.1	10.1	cg11827925;cg180	358	protein-coding	AQP1	aquaporin 1 (Colton blood group)		O	1.0	O	4.2		33.0	O	O
15204	31.1	33.2	8.6	cg14725537	5354	protein-coding	PLP1	proteolipid protein 1		O	1.1	O	3.6		24.6	O	O
15313	72.1	62.9	40.1	cg21573263	6536	protein-coding	SLC6A9	solute carrier family 6 (neurotransmitter transporter, glycine), member 9		O	1.1	O	1.8		32.0	O	O
15646	86.5	83.4	49.6	cg05548349	401562	protein-coding	LCNL1	lipocalin-like 1		O	1.0	O	1.7		36.9	O	O
16243	57.2	66.7	40.0	cg02458882;cg060	10133	protein-coding	OPTN	optineurin		O	1.2	O	1.4		26.7	O	O
16244	57.2	66.7	40.0	cg02458882;cg060	10133	protein-coding	OPTN	optineurin		O	1.2	O	1.4		26.7	O	O
16245	57.2	66.7	40.0	cg02458882;cg060	10133	protein-coding	OPTN	optineurin		O	1.2	O	1.4		26.7	O	O
16649	68.6	79.5	33.6	cg03704673	388323	protein-coding	GLTPD2	glycolipid transfer protein domain containing 2		O	1.2	O	2.0		45.8	O	O
16939	53.4	42.8	25.8	cg16715129;cg236	272	protein-coding	AMPD3	adenosine monophosphate deaminase 3		O	1.2	O	2.1		27.6	O	O
16940	57.0	55.9	35.9	cg16715129;cg239	272	protein-coding	AMPD3	adenosine monophosphate deaminase 3		O	1.0	O	1.6		21.1	O	O
17842	75.4	89.6	56.9	cg15255042	345930	protein-coding	ECT2L	epithelial cell transforming sequence 2 oncogene-like		O	1.2	O	1.3		32.7	O	O
17854	54.7	41.5	6.9	cg03309770;cg269	780776	protein-coding	FAM18A	family with sequence similarity 18, member A		O	1.3	O	8.0		47.9	O	O
18167	65.6	74.2	47.0	cg22148297	2841	protein-coding	GPR18	G protein-coupled receptor 18		O	1.1	O	1.4		27.2	O	O
18448	56.9	73.8	36.2	cg00556627;cg012	26010	protein-coding	SPATS2L	spermatogenesis associated, serine-rich 2-like		O	1.3	O	1.6		37.5	O	O
18450	56.9	73.8	36.2	cg00556627;cg012	26010	protein-coding	SPATS2L	spermatogenesis associated, serine-rich 2-like		O	1.3	O	1.6		37.5	O	O
18785	77.3	93.0	61.7	cg02634187	441054	protein-coding	C4orf47	chromosome 4 open reading frame 47		O	1.2	O	1.3		31.4	O	O
19202	77.4	80.3	52.7	cg01634964;cg023	6597	protein-coding	SMARCA4	SWI/SNF related, matrix associated, actin dependent regulator of chromatin, subfamily a, member 4		O	1.0	O	1.5		27.6	O	O
19335	50.7	68.3	43.4	cg04036101;cg040	3801	protein-coding	KIFC3	kinesin family member C3		O	1.3	O	1.2		24.9	O	O
19585	78.4	88.5	56.4	cg03392679;cg094	317649	protein-coding	EIF4E3	eukaryotic translation initiation factor 4E family member 3		O	1.1	O	1.4		32.1	O	O
19815	53.6	75.7	45.5	cg04956382;cg069	9499	protein-coding	MYOT	myotilin		O	1.4	O	1.2		30.2	O	O
20817	56.7	48.2	23.1	cg00964137;cg021	285600	protein-coding	KIAA0825	KIAA0825		O	1.2	O	2.5		33.6	O	O
21301	75.1	72.3	41.3	cg21463790	2115	protein-coding	ETV1	ets variant 1		O	1.0	O	1.8		33.8	O	O
21302	75.1	72.3	41.3	cg21463790	2115	protein-coding	ETV1	ets variant 1		O	1.0	O	1.8		33.8	O	O
21303	75.1	72.3	41.3	cg21463790	2115	protein-coding	ETV1	ets variant 1		O	1.0	O	1.8		33.8	O	O
21348	75.6	60.2	33.3	cg26367031	27094	protein-coding	KCNMB3	potassium large conductance calcium-activated channel, subfamily M beta member 3		O	1.3	O	2.3		42.3	O	O
21758	87.5	73.4	45.4	cg27446233	5213	protein-coding	PFKM	phosphofructokinase, muscle		O	1.2	O	1.9		42.1	O	O
21759	87.5	73.4	45.4	cg27446233	5213	protein-coding	PFKM	phosphofructokinase, muscle		O	1.2	O	1.9		42.1	O	O
21867	69.2	58.6	25.8	cg00412554;cg064	90293	protein-coding	KLHL13	kelch-like 13 (Drosophila)		O	1.2	O	2.7		43.5	O	O

【研究方法】

次に、多能性幹細胞の細胞規格方法として、ヒトES細胞とヒトiPS細胞のHuman Genome U133 plus 2.0を用いた網羅的遺伝子解析の結果より、遺伝子同士の関連性ネットワークをオミックス解析した。多能性維持に必要となる代表的な遺伝子群およびリプログラミング化で使用した遺伝子群を抽出し、ヒトES細胞に強く発現し、多能性維持を保持する因子(OCT3/4, NANOG, SOX2, KLF4 c-Myc, Lin28A) 間のネットワーク形成の様子と前遺伝子に加え、iPS細胞の樹立効率を向上させると報告されたGlis-1遺伝子を加えた遺伝子間のネットワーク形成の様子を比較した。（図4）

【結果】

Glis-1遺伝子の発現を経由するiPS細胞のシグナルは、NogginやBMP Familyのシグナル経路とリンクしていることを明示する判明、NANOGやPOU5F1など多能性維持遺伝子群のネットワーク構築とは直接的な関係性がないことが示唆された。従って分化誘導後でも残ると思われるGlis-1の恒常的

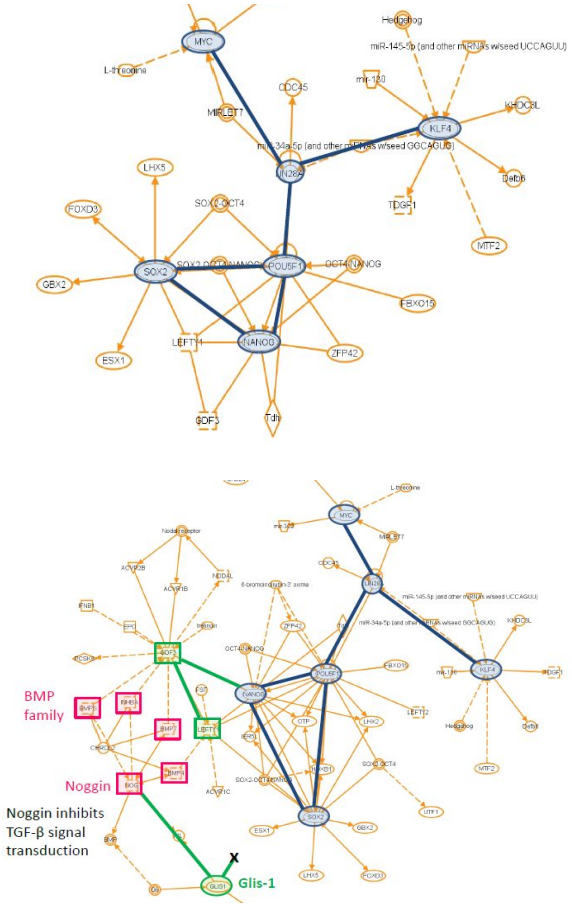

図4. 網羅的遺伝子発現データを用いたiPSC多能性維持ネットワーク(NW)解析.

上）リプログラミング化(POU5F1, NANOG, SOX2, Lin28A, KLF4, MCY)に利用されている主な遺伝子間のControllability analysis.
下) Glis-1 を追加した場合の遺伝子間のControllability analysis.

な発現は、分化誘導時にBMPやNonggginシグナルの恒常的な活性を促し、中胚葉系への誘導促進と特定の分化段階での分化阻害をもたらす可能性が示唆された。

一方、RPE細胞自身も単一細胞で低密度培養を行うことで比較的に緩和な培養条件下で中胚葉系細胞へと脱分化しやすいことが報告されている。[1)]

Glis-1をリプログラミング化に使用することで、Fibroblastや間葉系幹細胞(MSC)からiPS細胞の樹立効率が向上すると報告[2)]されているものの、ヒト臍帯血を細胞源とした場合では、Glis-1を導入した場合でも、iPS細胞の樹立効率の向上は認められなかった。つまり、iPS細胞の樹立条件は、細胞源のエピゲノム状態と密接な関係があり、Glis-1を使用した場合のリプログラミング化とGlis-1を使用しないリプログラミング化では、リプログラミング経路が異なる事が推察できる。Glis-1は、特定細胞種に存在する遺伝領域のリプログラミング化を促進する役割を示すものの、Glis-1を使用して樹立したiPS細胞では、Glis-1が残存した場合、BMPやNonggin シグナルの恒常的な活性を促し、中胚葉系への分化誘導の際は、中胚葉系中間体での分化異常細胞の出現が想定された。実際3次試験で出現した、MSCの性状と特性（脂肪、骨、軟骨分化）X細胞の出現は、このOmics解析で予見できる可能性が示唆された。

【考察】

Glis-1を用いて樹立したiPS細胞をRPEに分化誘導した3th RPE移殖組織片（非造腫瘍性分化中間体混入が著明なRPE細胞）で特異的に出現した（中胚葉系mesenchymal stem cell の性質を有した）細胞が、RPE細胞の脱分化系で起こるものかあるいは、iPS細胞のリプログラミングプロセスで発生するX細胞であるか、Omics解析を含めた多面的に検証することで、iPS細胞の分化抵抗性の予見や細胞規格化の検討が可能になることが考えられた。

参考文献）

1. Enrique Salero, et.al., “Adult Human RPE Can Be Activated into a Multipotent Stem Cell that Produces Mesenchymal Derivatives”., Cell Stem Cell, 10, 88–95 2012.

2. Momoko Maekawa, et.al. “Direct repro gramming of somatic cells is promoted by maternal transcription factor Glis1”, Nature, 474, 225-229, 2011.

【研究方法】

細胞あるいは組織から抽出した RNA を基に遺伝子網羅解析を行い、その遺伝子情報から iPS 細胞の品質をフィードバックすることが可能について評価検討した。まず、253G1 由来の RPE 細胞と Primary RPE 細胞から RNA を抽出し、Human Genome U133 plus 2.0 を用いて網羅的遺伝子解析データを行った。これらの遺伝子情報を代謝情報に変換しヒートマップを作成した。

【結果】

Primary RPE 細胞は、Protein Synthesis 代謝に関する遺伝子が多く発現していることが分かり、RPE 細胞自体が様々なタンパク質を分泌している特性を有することが確認できた。一方、iPS 細胞由来 RPE 細胞においても、Primary 細胞と同様に多くの Protein Synthesis 代謝の結果が見られた。その他、遺伝子発現から Cell Death and Survival や Cellular Growth and Proliferation に関する代謝発現も Primary RPE と iPS 細胞由来 RPE 細胞で同様の結果が得られた。（図 5）これらの結果より、iPS 細胞由来 RPE 細胞と PrimaryRPE 細胞の細胞内代謝状況は、非常に性質の近い細胞であることが確認された。

以上、移殖細胞や組織よりRNAを抽出し、遺伝子網羅解析を行う事により、iPS細胞由来分化細胞のさらなる細胞評価を行った。

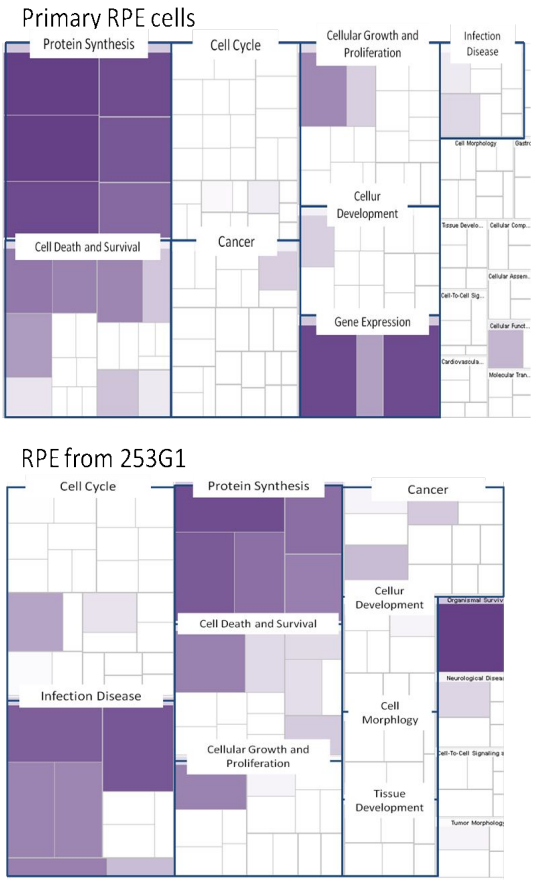

図 5. Primary RPE および 253G1 由来 RPE 細胞のオミックス解析での細胞内代謝の Heatmap

【研究目的】

細胞保管業務では、当初予想していた移殖細胞の保管だけでは有害事例発生時における細胞検査で十分な原因追究ができず再生医療の安全に推進するに繋がらない可能性が示唆されたことから、昨年度に作成した細胞情報管理、細胞保管場所管理、保管機器の監視、細胞保管施設の維持などに関する運用規定を、多種細胞の保管/管理する事を想定した運用規定および細胞保管/管理規定を改正し、多検体の保管が可能な運用方法の改正を行った。

【研究方法】

保管業務を遂行するために必要な契約書の管理やデータ・ホームページ管理、広報活動等の業務を支援するために事務局を設置し、必要人員を確保することでヒト幹細胞アーカイブの全体的な運用体制を確定した。

【結果】

細胞寄託に関する情報発信および細胞寄託時の個人情報管理等のヒューマンエラー防止、国民への広報活動のためヒト幹細胞アーカイブ【Archive of Human Stemcell in Clinical research; AHSC】用ホームページ (http://stemcell-archive.fbri.org) を作成し、次年度より医療機関ネットワークへの幹細胞の寄託依頼の手続きを開始する状況を整えた。また、細胞提供機関と寄託を受ける財団双方間で実運用のための契約締結準備中である。2014年3月には、臨床用細胞検体の保管シュミュレーションを実施し、運用マニュアル、管理マニュアルの最終確認を行った。ヒト幹細胞アーカイブ広報活動としては、細胞保管事業目的および細胞保管に対する契約内容（案）を理化学研究所 高橋政代先生らの細胞製造グループとMeetingし、細胞寄託について確認を頂いた(2012年11月11日)。

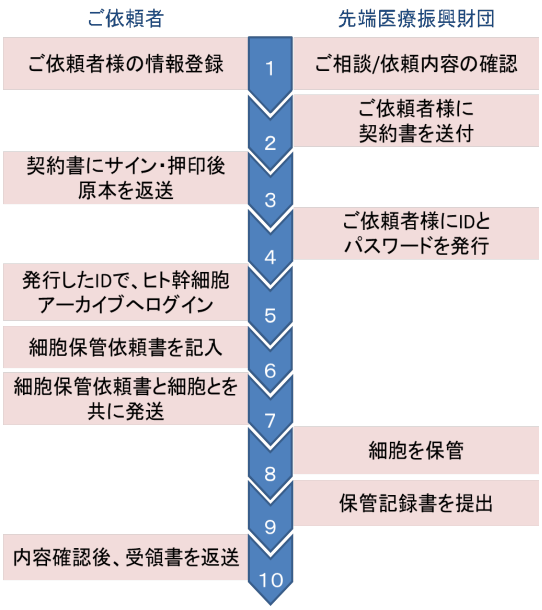

図6.　ヒト幹細胞アーカイブを活用した細胞保管業務のフローチャート*

***財団内のサーバーで公開型と非公開型に分類してセキュリティ面を担保しているため、細胞情報管理等の流れに関しては非公開しない。**

細胞保管事務局としては、細胞提供機関と細胞寄託に関する契約書の作成や細胞寄託に対する広報活動、ヒト幹細胞アーカイブ用ホームページの立ち上げを行い、ホームページ上に、細胞寄託者が細胞寄託するまでの手順をフローチャートとして明記し、容易に寄託依頼できるよう情報発信している。（図6）

細胞寄託までの操作

1. **細胞保管依頼者（以下；依頼者）にヒト幹細胞アーカイブ HP にアクセスして頂き、依頼者情報等を入力。**
2. **細胞保管事務局で依頼登録内容に問題がない事を確認後、依頼者に細胞保管業務委託契約書を発送する。**
3. **依頼者が契約書に捺印後、財団に返送。**
4. **契約締結を確認後、財団側で ID・パスワードを発行。**
5. **依頼者に ID・パスワードを送付する。**
6. **依頼者は、ID・パスワードでログインし、専用フォームの細胞情報記入欄を記入して、細胞発送日を指定する。**
7. **細胞保管事務局は、細胞受取り可能であることを確認し連絡する。**
8. **細胞を受け取り、細胞保管作業手順書に準じ細胞を保管する。**
9. **細胞情報に ID を付与し保管場所と細胞**保管記録書として保管する。
10. **細胞を受取り**
11. **依頼者に細胞保管受領書を送る。**

細胞保管施設の整備状況は、ES細胞/ iPS細胞の細胞保存用液体窒素タンク・超低温フリーザー・温度管理システム・室内酸素濃度センサー・検体管理システム整備を構築し、細胞保管機器の運転状況などの管理体制を整えた。(図7)

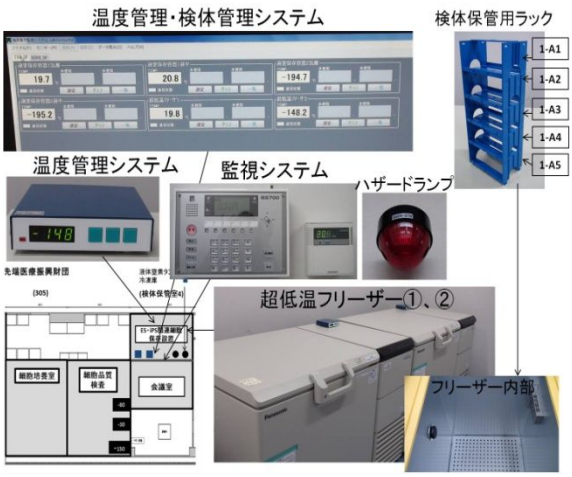

図7．細胞保管施設の整備状況

その他、Table 2 に示した各種規定書・手順書を作成した。

Table 2. 細胞保管保管情報の管理規定、手順書

1. 作業者の教育等の管理規定を設定。
2. 細胞保管事業に関する業務および契約規定、
3. 検体保管室管理規定 (受入細胞に関する入庫判定、入庫記録管理, 細胞保管不適合時の処置、細胞の取出し管理)
4. 検体保管室入室記録
5. 検体保管室の警戒発報に対する対応規定
6. 細胞保管場所アドレス入力規定
7. 検体保管室内細胞保管機器の作動監視規定
8. 検体保管依頼者の個人情報保護法の取り扱い規定
9. 検体保管依頼書の作成
10. 依頼蛮行発行規定
11. 検体情報の管理規定
12. 検体発送手順書の作成
13. 検体保管手順書の作成
14. 検体保管記録書の作成
15. 検体管理ID発行規定
16. 検体保管記録書の管理規定
17. セキュリティ侵害時の対応規定
18. 細胞返還依頼書の作成
19. ヒト幹細胞アーカイブのHP運用規定

【今後の予定】次年度には、慶応義塾大学中村雅也先生や京都大学　高橋淳先生らの

研究進捗に応じて、本事業への細胞寄託にご協力頂けるよう広報を行う予定である。具体的には、ヒト幹細胞アーカイブHPを活用し広報を行い細胞寄託を開始する。(図8)

広報活動としては、学術会議・シンポジウム・展示会等への出展を行い将来、臨床研究を実施される先生方への細胞寄託協力を求める。加えて、次年度に広報活動用としてヒト幹細胞アーカイブ用配布資料のA4 x 1 頁程度を作成する予定である。文部科学省「橋渡し研究」等の臨床研究実施、実施予定の先生方に配布資料を送付予定である。臨床研究 に使用されたiPS細胞由来RPE細胞の細胞寄託を開始。

次年度より、CGH array等を用いたCopy Numbers Variation (CNV)も染色体解析技術に導入し、gene stabilityと造腫瘍性に関する移植後検査法の開発に着手した。

図 8. ヒト幹細胞アーカイブの HP TOP 画面

平成25年度　厚生労働科学研究費補助金（難病・がん等の疾患分野の医療の実用化研究事業)

（再生医療関係研究分野）細胞保管事務局

細胞保管ホームページ立上に関する打合せ等

月日	時間	場所	参加者							主な内容
			(有)エムリンク　中山氏	(有)エムリンク　下氏	細胞療法開発事業部門　西氏	細胞療法開発事業推進課　清水	細胞療法開発事業推進課　ジェイ・コブ	細胞療法開発事業推進課　竹内	情報システム課　久後	情報システム課　大前	
H25年											
11月7日	14:00~15:30	TRI－2F 事務室	○	○	○		○	○			事業内容、HPの構想を(有)エムリンクに説明
11月15日	15:00~16:30	TRI－2F 事務室	○	○	○		○	○			(有)エムリンクよりHPコンテンツ概略(案)の提示
11月25日	13:30~14:30	IBR臨床棟3F 財団事務室			○		○	○	○	○	システム構成について、サーバ2台設置(公開用、DB用)。
12月5日	15:00~16:30	TRI－2F 西会議室	○	○		○	○	○	○	○	(有)エムリンクよりHPコンテンツ詳細(案)の提示、システム構成の確認
12月25日	16:00~16:30	TRI－2F 西会議室			○			○			事前打合せ
12月25日	16:30~17:30	TRI－2F 西会議室	○	C	C	C	C	C	C	C	(有)エムリンクよりHPコンテンツ修正(案)の提示、システム構成の再確認
H26年											
2月21日	10:00~11:00	TRI－2F 西会議室			○		○	○			HPコンテンツ、事務局とうボの役割分担
3月5日	11:30~12:30	TRI－2F 西会議室			○		○	○			HPコンテンツ確認→(有)エムリンクに修正依頼
3月10日	11:00~12:30	TRI－2F 西会議室			C		C	C			HPコンテンツ確認→(有)エムリンクに修正依頼
3月14日	10:00~11:00	TRI－2F 西会議室			○		○	○			HPコンテンツ確認→(有)エムリンクに修正依頼

OPEN ACCESS Freely available online

PLOS ONE

Tumorigenicity Studies of Induced Pluripotent Stem Cell (iPSC)-Derived Retinal Pigment Epithelium (RPE) for the Treatment of Age-Related Macular Degeneration

Hoshimi Kanemura[1,2], Masahiro J. Go[1], Masayuki Shikamura[1], Naoki Nishishita[1], Noriko Sakai[2], Hiroyuki Kamao[2,3], Michiko Mandai[2], Chikako Morinaga[2], Masayo Takahashi[2], Shin Kawamata[1,2]*

1 Division of Cell Therapy, Foundation for Biomedical Research and Innovation, Kobe, Japan, 2 Laboratory for Retinal Regeneration, RIKEN Center for Developmental Biology, Kobe, Japan, 3 Department of Ophthalmology, Kawasaki Medical School, Kurashiki, Okayama, Japan

Abstract

Basic studies of human pluripotential stem cells have advanced rapidly and stem cell products are now seeing therapeutic applications. However, questions remain regarding the tumorigenic potential of such cells. Here, we report the tumorigenic potential of induced pluripotent stem cell (iPSC)-derived retinal pigment epithelium (RPE) for the treatment of wet-type, age-related macular degeneration (AMD). First, immunodeficient mouse strains (nude, SCID, NOD-SCID and NOG) were tested for HeLa cells' tumor-forming capacity by transplanting various cell doses subcutaneously with or without Matrigel. The 50% Tumor Producing Dose (TPD_{50} value) is the minimal dose of transplanted cells that generated tumors in 50% of animals. For HeLa cells, the TPD_{50} was the lowest when cells were embedded in Matrigel and transplanted into NOG mice ($TPD_{50} = 10^{1.1}$, n = 75). The TPD_{50} for undifferentiated iPSCs transplanted subcutaneously to NOG mice in Matrigel was $10^{2.12}$; (n = 30). Based on these experiments, 1×10^{6} iPSC-derived RPE were transplanted subcutaneously with Matrigel, and no tumor was found during 15 months of monitoring (n = 65). Next, to model clinical application, we assessed the tumor-forming potential of HeLa cells and iPSC 201B7 cells following subretinal transplantation of nude rats. The TPD_{50} for iPSCs was $10^{4.73}$ (n = 20) and for HeLa cells $10^{1.32}$ (n = 37) respectively. Next, the tumorigenicity of iPSC-derived RPE was tested in the subretinal space of nude rats by transplanting $0.8–1.5\times10^{4}$ iPSC-derived RPE in a collagen-lined (1 mm×1 mm) sheet. No tumor was found with iPSC-derived RPE sheets during 6–12 months of monitoring (n = 26). Considering the number of rodents used, the monitoring period, the sensitivity of detecting tumors via subcutaneous and subretinal administration routes and the incidence of tumor formation from the iPSC-derived RPE, we conclude that the tumorigenic potential of the iPSC-derived RPE was negligible.

Citation: Kanemura H, Go MJ, Shikamura M, Nishishita N, Sakai N, et al. (2014) Tumorigenicity Studies of Induced Pluripotent Stem Cell (iPSC)-Derived Retinal Pigment Epithelium (RPE) for the Treatment of Age-Related Macular Degeneration. PLoS ONE 9(1): e85336. doi:10.1371/journal.pone.0085336

Editor: Alfred Lewin, University of Florida, United States of America

Received August 13, 2013; Accepted December 4, 2013; Published January 14, 2014

Funding: This study was supported by funding from JST research grant "Safety Tests for Pluripotent Stem Cell (2010–2014)" Japan. The funders had no role in study design, data collection and analysis, decision to publish, or preparation of the manuscript.

Competing Interests: The authors have declared that no competing interests exist.

* E-mail: kawamata@fbri.org

Introduction

Clinical cell therapy trials were recently initiated for treatment of Stargardt's disease and the dry type of age-related macular degeneration (dry AMD). The trials have used human embryonic stem cell (hESC)-derived retinal pigment epithelium (RPE) [1–4]. In addition, several groups are planning clinical trials with autologous human induced pluripotent stem cell (hiPSC)-derived RPE for the wet type of AMD. Thus, cell therapy using human pluripotent stem cells (hPSCs) has reached clinical application. However, in contrast to tissue stem cells that have a limited proliferation potential, tumor formation from residual undifferentiated or incompletely differentiated hPSCs in hPSC-derived cell products is an issue that must be carefully analyzed. This issue is particularly important when transplanting autologous hiPSC-derived cells.

We recently reported a highly sensitive residual hiPSC detection method based on qRT-PCR using primers for the LIN28A transcript [5] in hiPSC-derived RPE. This method enables us to detect residual hiPSCs down to 0.002% of differentiated RPE cells. As we plan to transplant $4–8\times10^{4}$ hiPSC-derived RPE cells into the subretinal space of patients, this method is sensitive enough to detect a few residual hiPSCs, if any, in a clinical setting.

The tumorigenic potential of hiPSC-derived RPE cells is attributable to contamination by undifferentiated hiPSCs, intermediate products having proliferation potentials and/or tumorigenic transformed cells. Contamination by these cells should be assessed by nonclinical testing using suitable animal models [6,7]. However, there is no internationally recognized guideline for tumorigenicity testing in cell therapy products. The most relevant guideline is the WHO TRS 878, ''Recommendation for the evaluation of animal cell cultures as substrates for the manufacture of cell banks'' [8,9]. The guideline recommends transplanting 1×10^{7} test cells subcutaneously to 10 nude mice and monitoring tumor formation for more than 16 weeks. Transplantation of the same dose of a well-known tumorigenic cell line such as HeLa in parallel is suggested as a tumor-forming positive control. The WHO guideline covers animal cell substrates for the production of

biological medicinal products and specifically excludes viable animal cells that are intended for therapeutic transplantation into patients. To examine the tumorigenicity of hiPSC-derived cells intended for administration to patients, several teratoma-forming tests exploring dose and administration route were studied using immuno-deficient mice [6],[10]. However, discussions how we can interpret and extrapolate the results of tumorigenicity testing with immuno-deficient or immuno-suppressant animals to human patients continue [6,7]. Recently a commentary report from FDA/CBER pointed out the issues to be considered for cell-based products and associated challenges for preclinical animal study [11]. The report stated that although the nature of cells used for cellular therapy is diverse, tumorigenic test results from the administration of cells through nonclinical routes would not be considered relevant as it would not track the behavior of transplanted cells in a micro-environment. When tumorigenicity testing of ESC-derived cellular products is undertaken, the study design should include groups of animals that have received undifferentiated ESCs, serial dilutions of undifferentiated ESCs combined with ESC-derived final products and the final intended clinical products. This approach would thereby address the tumor-forming potential of these cell groups in animal models.

Tumorigenicity testing via the clinical route of administration could recapitulate the fate of transplanted cells in a microenvironment of host tissue and could be fairly extrapolated to human application. However, elaborate surgical intervention requires skills that greatly influence the outcome of transplantation. For example, it is difficult to determine whether the cells were transplanted into the right location or organ in small rodents. These concerns can be overcome by conducting a subcutaneous tumorigenicity test in addition to testing via the clinical route.

In this report, we conducted 2 types of in vivo tumorigenicity tests by transplanting hiPSC-derived RPE cells into subcutaneous and sub-retinal spaces in immuno-deficient animals. The results and limits of these tests are discussed.

Results

Tumorigenicity Tests with Several Types of Immuno-deficient Mice

The tumor-forming potential of human iPSC-derived cell products should be examined using a suitable animal transplantation model. One should take into account the number of cells to be transplanted, the method of transplantation, the microenvironment of the transplantation site, the monitoring period and the status of the immune-deficient animals.

First, we checked the tumor-forming potential of several immune-deficient animals by subcutaneously transplanting HeLa cells over a wide range of doses (1 to 1×10^6 in 10-fold increments) with or without Matrigel (BD) and observed tumor formation every day for up to 36 weeks on a daily basis. Matrigel is known to enhance the tumor-forming potential of transplanted cells [16]. Recipient animals included immune-deficient nude, SCID [10], NOD-SCID [17], and NOG [18] mice. The minimal dose of transplanted cells that generated tumors in 50% of the transplanted animal (TPD_{50}) was calculated statistically to evaluate the sensitivities of tumor formation in each animal model [19]. We found the NOG mouse was most susceptible to tumors. That is, when transplanted subcutaneously with Matrigel, tumors were generated by the lowest number of HeLa cells. The TPD_{50} for HeLa was $10^{1.1}$ (n = 75), in agreement with a previous report [20], (Figure 1, Table 1). It is interesting to note that among the conditions tested, the highest number of HeLa cells was required to form tumors in nude mice without Matrigel. TPD_{50} for nude mice without Matrigel was $10^{4.9}$ (n = 120), which is also in agreement with a previous report [19] (Figure 1, Table 1). Therefore, we selected NOG mice and Matrigel for embedding the test cells for further assays as it provided sensitive tumor detection using small numbers of transplanted cells. The tumor-formation potential of iPSCs was assessed by subcutaneously transplanting several doses of the iPSC cell line 201B7 with Matrigel into NOG mice. The TPD_{50} for iPSC was $10^{2.12}$ (n = 30) over 12 months' monitoring (Table 2). The TPD_{50} value for iPSCs in subcutaneous transplantation provided a reference cell number for the contamination of iPSCs in iPSC-derived RPE cells.

Characterization of Established hiPSCs and hiPSC-derived RPE

hiPSC lines 59-G3, 101-EV3, K11-EV9, K21-EV15 K21-G18, 101-G25, RNT9-2-8, and RNT10–24 were established from dermal fibroblasts of 6 patients (59, K11, K21, 101, RNT9, RNT10) with retinitis pigmentosa. Quality control tests for established iPSCs were as follows. (1) Cells form colonies and must show human ESC-like morphology by microscopic observation. (2) Cells must express SSEA-4, TRA-1-60, POU5F1 (OCT3/4) and NANOG proteins as determined by immunostaining. (3) Cells must not express EBNA plasmid fragment by PCR or qRT-PCR. (4). Cells must possess a normal karyotype by the G-band method.

Retinal differentiation was subsequently initiated. The resulting RPE cell lines were established as follows. 59-G3 RPE was derived from hiPSC clone 59-G3; 101-EV3 RPE was from 101-EV3; K11-EV9 RPE was from K11-EV9; K21-EV15 RPE was from K21-EV15; K21-G18 RPE was from K21-G18; 101-G25 RPE and RNT9 RPE were from RNT9-2-8; and, RNT10 RPE was from RNT10-24. The protocol for RPE differentiation from hiPSC was shown in our recent report [21]. It requires 3 months for RPE differentiation and another 2 months to prepare the RPE sheet. The following quality control tests for the hiPSC-derived RPE cell lines were conducted. (1) The EBNA plasmid fragment was not detectable by PCR. (2) The cells showed the characteristic morphology and pigmentation of RPE with a single or double layer cell structure. (3) BEST1 and PAX6 molecules were detected by immunohistochemistry in over 95% of final hiPSC-derived RPE cells. (4) RPE-specific markers RPE65, CRALBP, MERTK and BEST1 were confirmed by RT-PCR. (5) LIN28A was not detected by qRT-PCR. (6) Migration of non-RPE cells into the collagen layer lining the hiPSC-derived RPE cell sheet shall be below 0.1% of the total RPE cells. (7) The RPE cell sheet shall consist of over 70% viable cells with a density of over 4500 cells/mm^2. Items (6) and (7) were quality control tests for the RPE cell sheet. All the cell culture processes including establishment of hiPSCs from a patient's fibroblasts and differentiation to RPE were conducted in a GMP-grade cell processing facility. The morphology and immunostaining of hiPSC-derived RPE cell lines 59-G3 RPE, K21-G18 RPE and 101-G25 RPE are shown in Figure 2A, B. The other hiPSC-derived RPE cell lines showed the same phenotype. The gene expression patterns of these cell lines are shown in Figure 2C. Primary RPE was used as a reference. It is notable that neither LIN28A nor POU5F1 (OCT3/4) was detected above background levels in hiPSC-derived RPE cells[5]. This finding serves as a useful criterion to eliminate immature hiPSCs in hiPSC-derived RPE (Figure 2D, 2E).

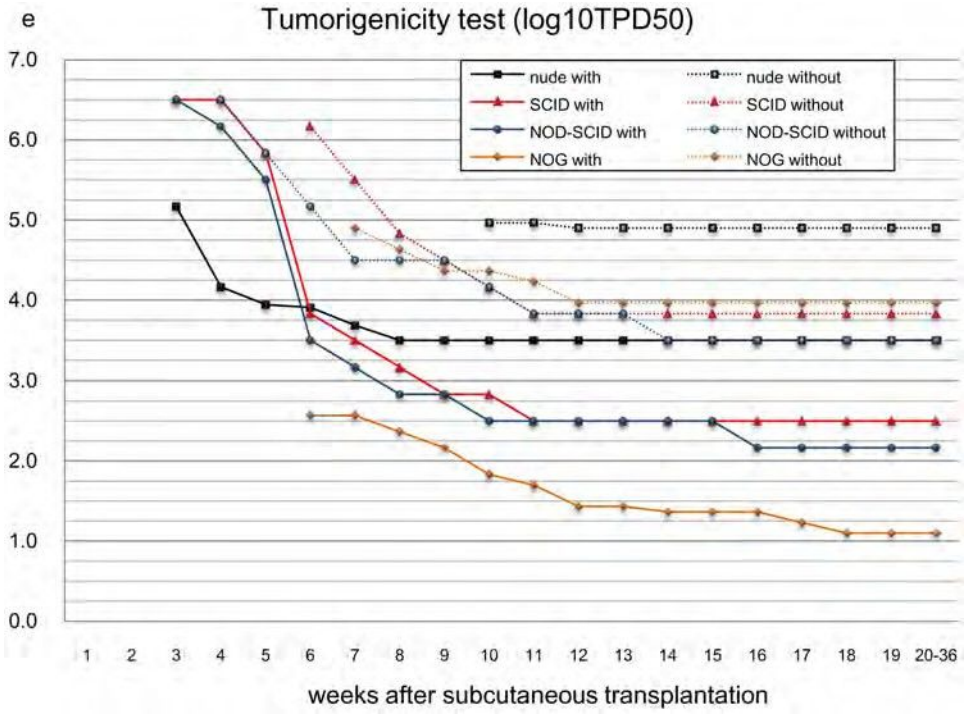

Figure 1. Tumorigenicity testing (TPD_{50} log_{10}) by subcutaneous transplantation of HeLa cells. $Log_{10}TPD_{50}$ values (minimal cell doses for 50% of animals to form a tumor) for HeLa cells when transplanted subcutaneously in various immuno-deficient mouse strains (nude, SCID, NOD-SCID, NOG) with or without Matrigel as indicated. Abscissa, weeks after transplantation. Ordinate, Log_{10} TPD_{50} values, logarithmic scale.
doi:10.1371/journal.pone.0085336.g001

Tumorigenicity Testing of hiPSC-derived RPE (Subcutaneous Transplantation)

To assess the tumorigenic potential of hiPSC-derived RPE cells with high sensitivity, subcutaneous transplantation of a large number of RPE cells would be ideal. However, the maximal number of RPE cells available for transplantation was limited by the culture capacity of the cell processing facility. We hypothesized that transplanting 1×10^6 hiPSC-derived RPE cells was an acceptable cell number to address the tumorigenic potential of the final cell product when embedded in Matrigel in NOG mice. This hypothesis was based on the facts that we expect to transplant 4–8×10^4 hiPSC-derived RPE in a clinical setting and as few as 10 undifferentiated hiPSCs or HeLa cells embedded in Matrigel could generate tumors in NOG mice (Table 1, Table 2).

Thus, we subcutaneously transplanted 1×10^6 hiPSC-derived RPE cells embedded in Matrigel into NOG mice [total n = 42; 59-G3 RPE (n = 14), K21-G18 RPE (n = 13), 101-G25 RPE (n = 15)]. Tumor formation was monitored for more than 70 weeks. Teratoma derived from subcutaneously transplanted iPSCs was analyzed as a positive control for tumor formation event (Figure 3A–3E). The proliferative status of living cells was assessed by HE, Hoechst 33258 and anti-Ki67 antibody staining (Figure 3G–3I). iPSC-derived neural rosette-like human cells were stained by anti-Lamin A antibody to check the specificity of anti-Lamin A antibody for human cells (Figure 3F). We assumed that

Table 1. Incidence of tumor formation after transplanting HeLa cells in various immunodeficient mice.

strain	use of Matrigel	min.dose for tumor formation	weeks to observe Tumor (first to last)	number of mice	Log10TPD50
nude	with	1×10^4 cells	3 to 8	120	3.5
nude	w/o	1×10^4 cells	4 to 12	120	4.9
SCID	with	1×10^3 cells	3 to 11	24	2.5
SCID	w/o	1×10^3 cells	3 to 11	24	3.83
NOD-SCID	with	1×10^2 cells	3 to 16	24	2.17
NOD-SCID	w/o	1×10^3 cells	3 to 14	24	3.5
NOG	with	1×10^1 cells	5 to 18	75	1.1
NOG	w/o	1×10^4 cells	3 to 13	105	3.97

$Log_{10}TPD_{50}$ values for HeLa cells transplanted subcutaneously into various immunodeficient mouse strains with or without Matrigel. Tumor-forming potentials of HeLa cells in nude mice without Matrigel and in NOG mice with Matrigel are highlighted in gray.
doi:10.1371/journal.pone.0085336.t001

Table 2. Tumorigenicity testing by subcutaneous transplantation of hiPSC-derived RPE into NOG mice.

hiPSC cell line	cell form	min.dose for tumor formation	weeks to observe Tumor (first to last)	number of mice	Log10TPD50
201B7	Cell suspension in Matrigel	1×10^1 cells	5–40	30	2.12
RPE cell line	**cell form**	**number of cells transplanted**	**monitor period**	**number of mice**	**tumor formation**
59-G3(1)	RPE cell suspension in Matrigel	1×10^6 cells	26–84 weeks	9	none
K21-G18	RPE cell suspension in Matrigel	1×10^6 cells	26–74 weeks	8	none
101-G25	RPE cell suspension in Matrigel	1×10^6 cells	23–70 weeks	10	none
59-G3(1)	RPE cell sheet in Matrigel	1×10^6 cells	28–85 weeks	5	none
K21-G18	RPE cell sheet in Matrigel	1×10^6 cells	13–79 weeks	5	none
101-G25	RPE cell sheet in Matrigel	1×10^6 cells	23–79 weeks	5	none
primary RPE	Cell suspension in Matrigel	1×10^6 cells	52 weeks	3	none
primary RPE	Cell suspension w/o Matrigel	1×10^6 cells	52 weeks	2	none
59-G3(2)	RPE cell sheet in Matrigel	1×10^6 cells	26–50 weeks	3	none
RNT10	RPE cell sheet in Matrigel	1×10^6 cells	26–46 weeks	3	none
RNT9	RPE cell sheet in Matrigel	1×10^6 cells	26–38 weeks	3	none
101-EV3	RPE cell suspension in Matrigel	1×10^6 cells	39 weeks	5	none
K11-EV9	RPE cell suspension in Matrigel	1×10^6 cells	39 weeks	3	none
K21-EV15	RPE cell suspension w/o Matrigel	1×10^6 cells	39 weeks	4	none
K11-EV9	RPE cell suspension w/o Matrigel	1×10^6 cells	39 weeks	2	none

$Log_{10}TPD_{50}$ value for hiPSC 201B7 determined by subcutaneously transplanting cells in Matrigel into NOG was calculated by the Trimmed Spearman-Karber method (upper panel). Tumor formation from 1×10^6 hiPSC-derived RPE cells prior to making RPE sheets (cell suspension) or after making RPE sheets (cell sheet) transplanted subcutaneously in various conditions into NOG mice. Animals were monitored for 13–85 weeks (lower panel).

doi:10.1371/journal.pone.0085336.t002

anti-human Lamin A antibody could stain a wide range of human cell types and was not limited to human RPE. Transplantation of 1×10^6 primary RPE cells embedded in Matrigel (n = 3) was used as a transplantation control. No tumor formation was observed from transplanted 1×10^6 hiPSC-derived RPE of several origins in various administration forms. All of the subcutaneous tumorigenicity tests conducted for hiPSC-derived RPE under various conditions using NOG mice are shown in Table 2.

All subcutaneous transplants consisting of RPE cells embedded in Matrigel were excised and subjected to histological examination. The size of transplants in subcutaneous tissue (Figure 4A, 4B) was similar to that of Matrigel without RPE (Figure 4C). Histological and immunohistological study showed that Lamin A-, BEST1- and Hoechst-positively staining RPE cells were present in all the Matrigel transplants (Figure 4F–4M). None of the cells transplanted in Matrigel stained with anti-Ki67 antibody, suggesting the absence of active proliferation in these transplanted cells (Figure 4D, 4E). Human cells derived from transplanted iPSC-derived RPE could be detected by Alu PCR at a level of $\geq$0.1% in mouse cells. However, we could not detect human cells in subcutaneous mouse tissue just beneath the transplants, in liver, spleen, kidney or lung by this method (Figure 5A, 5B).

Tumorigenicity Test of hiPSC-derived RPE (Subretinal Transplantation)

Next, we conducted tumorigenicity tests by transplanting test cells into the subretinal space, a procedure that is technically demanding. We chose large albino nude rats to facilitate transplantation and minimize variability of test results. This choice also permitted us to transplant larger doses of human hiPSC-derived RPE cells to the subretinal spaces. First, we assessed the tumor-formation potential of HeLa and iPSC 201B7 via subretinal transplantation. The TPD_{50} for HeLa was $10^{1.32}$ (n = 37) and $10^{4.73}$ for iPSC (n = 20) (Table 3). Teratomas derived from subretinally transplanted iPSC or tumors derived from transplanted HeLa cells were analyzed as positive controls for tumor formation event in the subretinal space (Figure 6A–6I). The proliferative status of living cells was assessed by HE, Hoechst 33258 and anti-Ki-67 antibody staining (Figure 6J–6L). iPSC-derived human cells were stained by anti-Lamin A antibody to check the specificity of anti-human Lamin A antibody to human cells (Figure 6M–6O).

Next, we conducted tumorigenicity tests of iPSC-derived RPE by transplanting 1 mm^2-sized (1 mm$\times$1 mm) iPSC-derived RPE sheets consisting of $0.8–1.5\times10^4$ RPE cells into the subretinal space of nude rats (n = 26). The RPE cell number was assessed by cell density and sheet size transplanted. Considering the relative sizes of humans and rats, we estimated that transplanting 0.8–1.5×10^4 RPE cells into the subretinal space of nude rats would provide the information required to determine the incidence of tumor formation in humans, as we expect to transplant 4–8×10^4 RPE cells in a clinical setting. Thus, we transplanted 5 different hiPSC-derived RPE cell sheets from 5 different patients to minimize individual variations. hiPSC-derived RPE sheets [59-G3 RPE (n = 9), K21-G18 RPE (n = 4), 101-G25 RPE (n = 3), RNT9 RPE (n = 5), RNT10 RPE (n = 5)] were prepared and transplanted under various conditions. Transplanted nude rats were monitored for tumor formation and physical condition daily for 8 to 82 weeks.

No tumor was found during the period of observation (Table 3). All transplanted eye balls were excised and subjected to histological examination. The location of transplanted RPE sheet

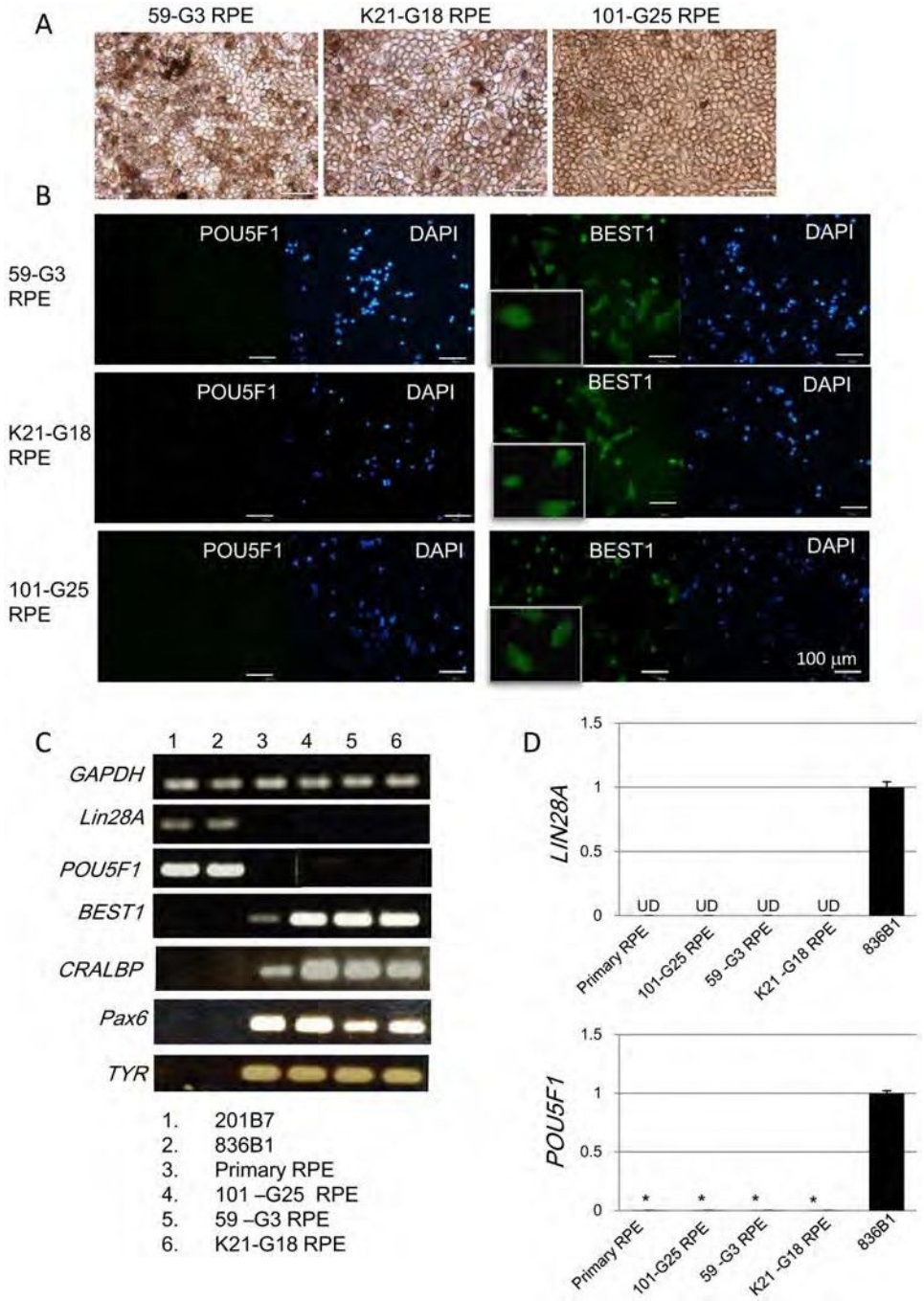

Figure 2. Characterization of hiPSC-derived RPE. A: Phase contrast images of hiPSC-derived RPE cell lines 59-G3 RPE, K21-G18 RPE and 101–G25 RPE. B: Expression of pluripotency-related molecules POU5F1 (OCT3/4, upper panels) and RPE-related molecules BEST1 (lower panels) in lines 59-G3 RPE, K21-G18 RPE and 101–G25 RPE as detected by immunostaining with specific antibodies. Nuclei were stained with DAPI. Magnified photos of BEST1 staining are appended in left lower corners. C: Gene expression profiles of hiPSC-derived RPE cell lines 59-G3-RPE, K21-G18 RPE, 101-G25 RPE. Expression of pluripotent stem cell-related gene markers LIN28A and POU5F1, or RPE-related makers BEST1 (bestrophin), CRALBP, PAX6 and TYR (tyrosinase) in hiPSC cell lines 201B7 and 836B1, primary RPE (hRPE-1) and hiPSC-derived RPE cell lines 59-G3 RPE, K21-G18 RPE, 101-G25 RPE as determined by RT-PCR (left panel). GAPDH was used as an internal control. 50 ng RNA was used for one RT reaction. Gene expression of LIN28A (D) or POU5F1 (E) in hiPSC-derived RPE cell lines 59-G3 RPE, K21-G18 RPE, 101-G25 RPE, hiPSC 836B1 and primary RPE was quantified by qRT-PCR. UD: undetectable level (D). *, $P \gtrsim 0.005$ (E). P values for primary RPE, 101-G25 RPE, 59-G3 RPE, or K21-G18 RPE versus 836B1 are 0.000153, 0.000177, 0.000432 or 0.000489, respectively.
doi:10.1371/journal.pone.0085336.g002

was shown by the brown color of the RPE sheet in albino nude rats (Figure 7A–7B). Histological and immunohistological studies showed that Lamin A- and Hoechst-positively staining or BEST1- and Hoechst-positively staining transplanted RPE cells were present in the subretinal space (Figure 7H–7O). Although we used serial sections for this staining, we believe more than half of Lamin A positive-human cells were stained with Hoechst, suggesting that these cells were live human transplanted cells at

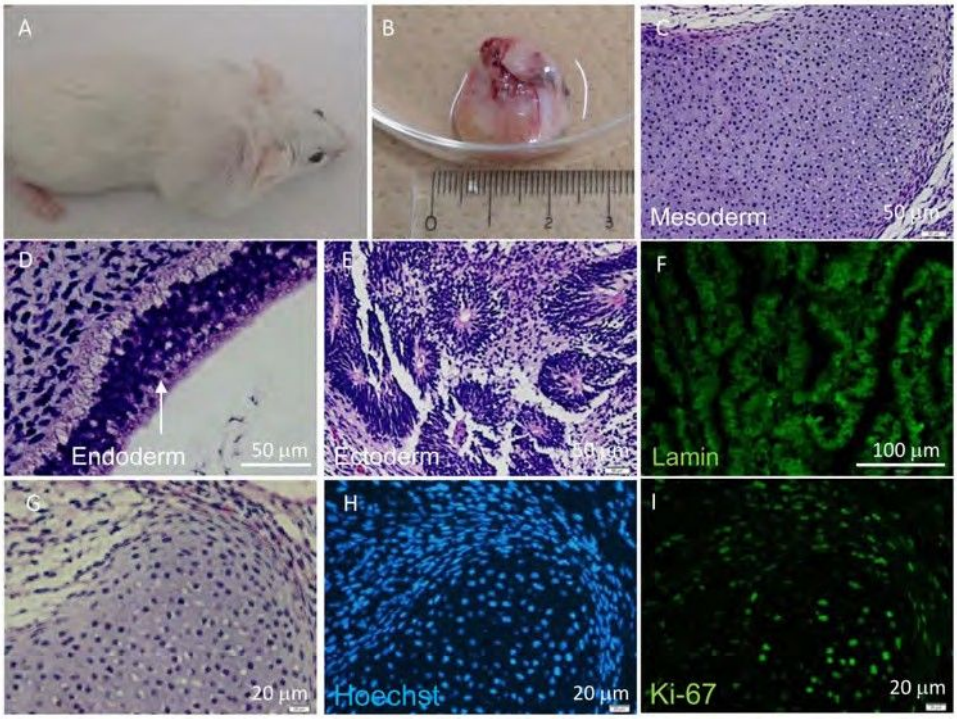

Figure 3. Histological analyses of hiPSCs subcutaneously transplanted into NOG mice. Tumor (teratoma) in NOG mouse was detected 5 weeks after transplanting 1.0×10^4 hiPSCs embedded with Matrigel (A, B). HE staining of sectioned hiPSC-derived teratoma consisted of three germ layers: cartilage-like tissue (mesoderm) (C), intestinal epithelium-like tissue (endoderm) (D) and neural rosette-like tissue (ectoderm) (E). Anti-Lamin A antibody (F) staining of rosette-like tissue. HE (G), Hoechst 33258 (H) and anti-Ki-67 antibody (I) staining of cartilage-like tissue.
doi:10.1371/journal.pone.0085336.g003

the end of the experiment (Figure 7H–7K). However, none of the cells in the sub-retinal space was stained with anti-Ki-67 antibody, suggesting that there was no ongoing proliferation in transplanted RPE cells (Figure 7D–7G). Histological analysis of serial sections showed that the shape of hiPSC-derived RPE sheet was maintained after transplantation and no evidence of tissue invasion or destruction of the vicinity of retinal structure was observed (Figure 7C, 7D).

Discussion

Here, we presented the results of nonclinical tests assessing the tumorigenic potential of hiPSC-derived RPE sheets. These studies represent a portion of the nonclinical testing of our scheduled clinical study for the use of autologous hiPSC-derived RPE sheets for the treatment of wet type AMD. The clinical study is scheduled to commence in 2014. The hiPSC-derived RPE cells used in this study were prepared in a GMP-grade cell processing facility using the same procedures that will be used for patient treatment.

Two types of tumorigenicity tests are summarized in this report. The first was a subcutaneous tumorigenicity test in NOG mice using Matrigel and the second was a subretinal tumorigenicity test in nude rats. It is intriguing to compare the objectives and the validity of the 2 tests in regard to hiPSC-derived RPE cell transplantation. Rationales for conducting subcutaneous tumorigenicity test are as follows:

1. Large numbers of test cells can be transplanted without difficulty, and bias-inducing variations in technical skills can be neglected. Moreover, the tumors are easy to detect. Therefore, statistical and endpoint analysis (TPD_{50} assessment) can be conducted in a timely and accurate manner.
2. It is possible to conduct comparison studies of the tumor-forming potential of different cellular products under the same transplantation conditions.
3. Above all, this test could serve as a substitute for in vitro soft agar assays of PSCs. PSCs cannot survive in soft agar, so that mode of testing is not feasible [5]. In contrast, PSCs or PSC-derived cells can survive long-term (more than 12 months) in Matrigel when subcutaneously transplanted in NOG mice. We can detect tumors derived from as few as 10 iPSCs or HeLa cells in this system (Table 1, Table 2). Thus, it provides a highly sensitive tumorigenic test for detecting both residual hiPSCs and tumorigenic transformed cells in hiPSC-derived cell products.

In this context, subcutaneous transplantation testing can be considered a quality control test of final cell products to ensure the absence of tumorigenic cells rather than characterizing the tumorigenic potential of the final cell products at a clinical transplantation site.

Next, we conducted tumorigenicity tests of hiPSC-derived RPE via clinical administration route. Under physiological conditions, the RPE is a monolayer that secretes various cytokines to maintain its structure in the retina. Diniz et al [3] reported that RPE transplanted in sheets retain better survival than when transplanted in suspension. For clinical application, we plan to transplant hiPSC-derived RPE in a sheet form and our preclinical testing was designed accordingly. Although we do not have RPE cell survival data in suspension form, it would be logical to presume that the transplantation of RPE in a sheet form exerts physiological function more effectively than in suspension, which may also facilitate the adaption of transplanted cells to the subretinal tissues.

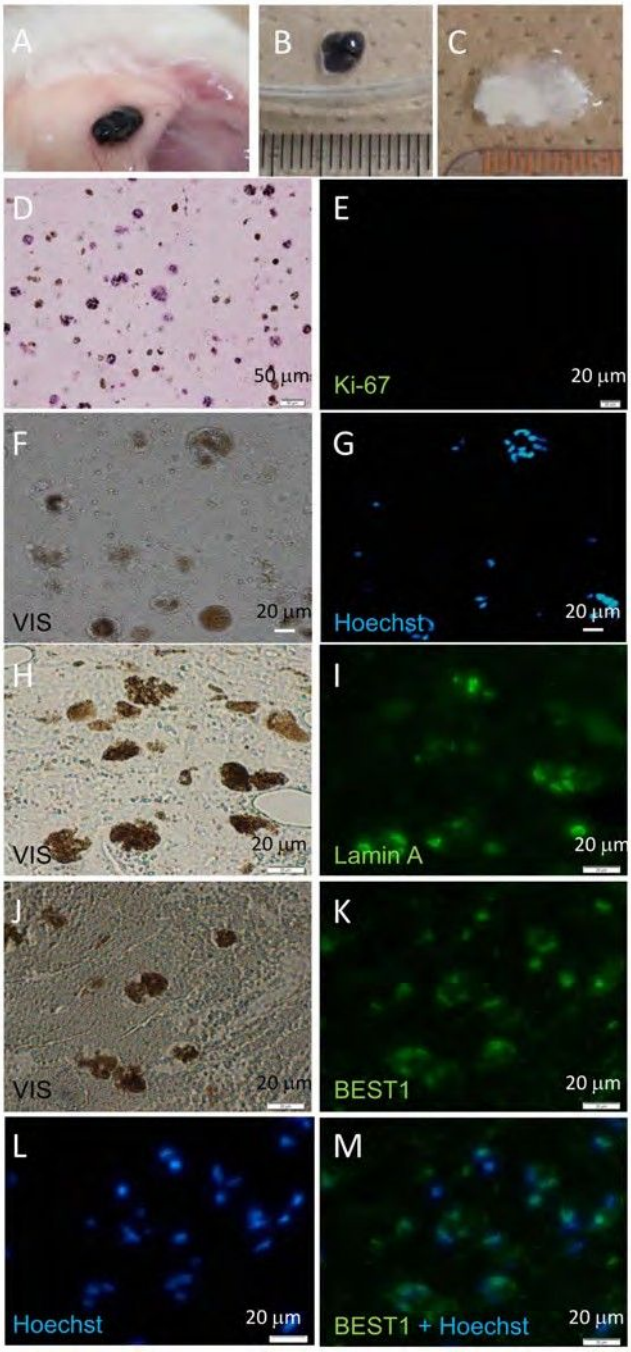

Figure 4. Histological analysis of hiPSC-derived RPE transplanted subcutaneously into NOG mice. NOG mice were examined six months after transplantation of 1.0×10^6 hiPSC-derived RPE cells in Matrigel into subcutaneous tissue. No tumor was detected visually. Site of transplant (A), excised transplant (B), and excised Matrigel only transplant (Matrigel without RPE cells C). Transplants were sectioned and stained with HE (D) and anti-Ki67 antibody (E). Photomicrograph of unstained serial section (F), and section stained with Hoechst 33258 (G). Photomicrograph of unstained serial section (H) or stained with anti-Lamin A antibody (I). Photomicrograph of unstained serial section (J) or stained with anti-BEST1 antibody (K) and Hoechst 33258 (L) and merged (M). Ki-67 positive cells were not observed.
doi:10.1371/journal.pone.0085336.g004

With regard to the tests' ability to detect immature (undifferentiated) hiPSCs in the subretinal space as a growing tumor, we

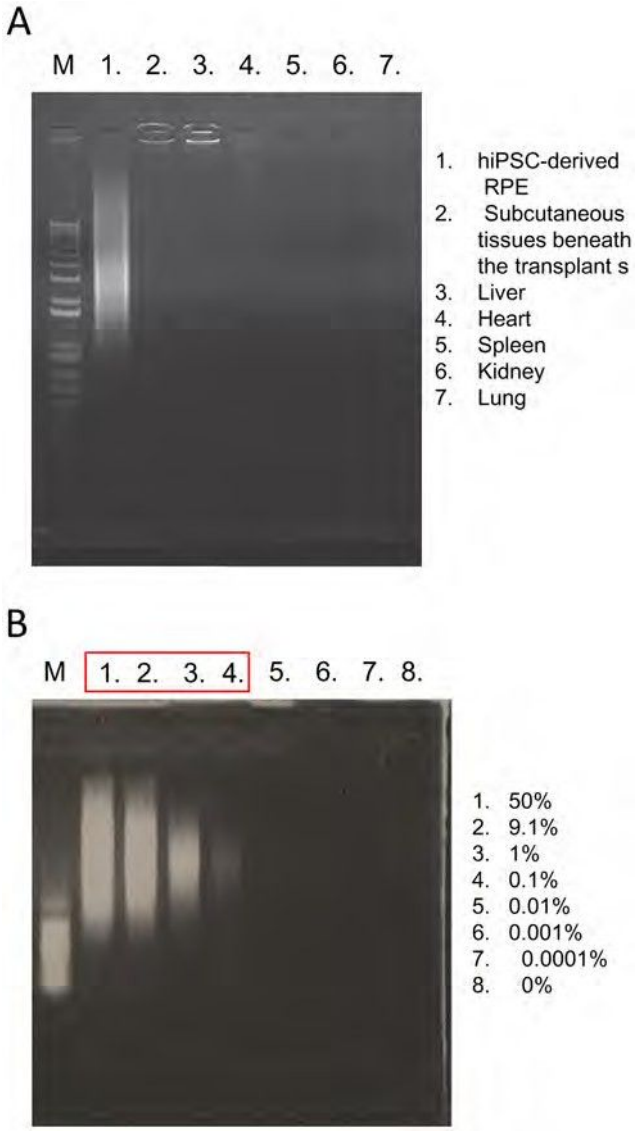

Figure 5. Detection of human cells in host mouse tissue by Alu PCR. DNA from hiPSC-derived RPEs (positive control, Lane 1), NOG mouse subcutaneous tissue just beneath the transplants (2), mouse liver (3), mouse heart (4), mouse spleen (5), mouse kidney (6) and mouse lung (7) were used as PCR templates. M: 1 kb marker (A). Alu PCR detects $\leq$0.1% human cells included in mouse cells determined by visual assessment of PCR products generated from various ratios of human: mouse DNA template mixtures. Percentage of human DNA in DNA mixture is shown in a respective lane number (1–8) (B). M: 1 kb marker.
doi:10.1371/journal.pone.0085336.g005

demonstrated the trans-effects of RPE on hiPSC in our recent studies. We reported that RPE secreted pigment epithelium derived-factor (PEDF) that markedly induced apoptosis in hiPSC and hESC [21]. hiPSCs or ESCs in culture inserts ceased to survive when co-cultured with RPEs. Further addition of hPEDF induced apoptosis in hiPSCs or ESCs drastically. In fact, when hiPSCs were transplanted into the subretinal space of nude rats, the $\log_{10}TPD_{50}$ value was 4.73 (n = 20), whereas the value was only 2.12 (n = 30) when hiPSCs alone were transplanted subcutaneously into NOG mice with Matrigel. The 400-fold difference in the TPD_{50} values under these conditions are at least partly explained by an environmental effect related to the subretinal

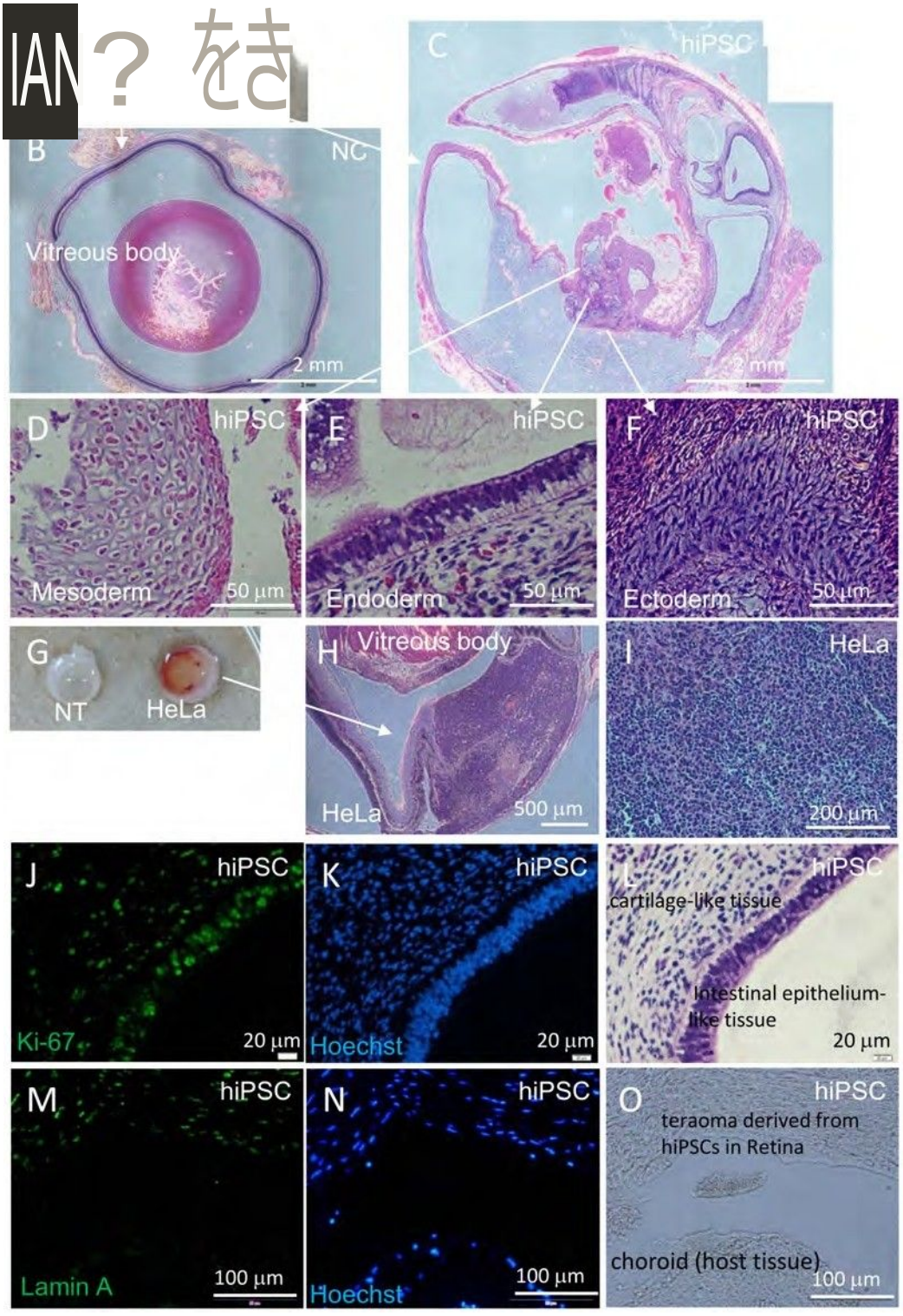

Figure 6. Histological analyses of hiPSCs or HeLa cells transplanted into the subretinal space of nude rats. Eye balls were excised from a nude rat 7 weeks after subretinal transplantation of hiPSC. Non-transplanted right eye ball (ND and left eye ball transplanted with 1 x10 hiPSCs (hiPSC) (A). HE staining of cross section of NT eye ball (B) and hiPSC-transplanted eye ball (C). HE staining of hiPSC-derived teratoma with three germ layers: cartilage-like tissue (mesoderm, D), intestinal epithelium-like tissue (endoderm, E) and neuron-like tissue (ectoderm, F) in hiPSC-transplanted eye ball. (G–O) Eye balls were excised from a nude rat 5 weeks after subretinal transplantation of Hela cells. Non-transplanted right eye ball (ND and left eye ball transplanted with 1 x 10^5 Hela cells (Hela) (G). HE staining of cross section of Hela cell-transplanted eye ball (H) and Hela-derived tumor tissue (I). Anti-Ki-67-antibody (J), Hoechst 33258 (K) and HE staining (l) of serial sections of hiPSC-derived teratoma. Anti-lamin A antibody (M), Hoechst 33258 staining and microscopic image (O) of serial cross sections containing a boundary of hiPSC-derived teratoma and host rat tissue. Anti-lamin A antibody specifically recognizes human cells in rat tissue.

doi:10.1371/journal.pone.0085336.g006

Table 3. Tumorigenicity testing by subretinal transplantation of hiPSC-derived RPE in nude rats.

hiPSC cell line	cell form	min.dose for tumor formation	weeks to observe Tumor (first to last)	number of rats	Log10TPD50
HeLa	Cell suspension w/o Matrigel	1×10^1 cells	5–33	37	1.32
hiPSC 201B7	Cell suspension w/o Matrigel	1×10^4 cells	7–33	20	4.73
RPE cell line	**cell form**	**number of cells transplanted**	**monitor period**	**number of rats**	**tumor formation**
59-G3 (1)	RPE cell sheet w/o Matrigel	$0.8–1.5\times10^4$ cells	9–82 weeks	4	none
K21-G18	RPE cell sheet w/o Matrigel	$0.8–1.5\times10^4$ cells	9–82 weeks	4	none
101-G25	RPE cell sheet w/o Matrigel	$0.8–1.5\times10^4$ cells	9–82 weeks	3	none
59-G3 (2)	RPE cell sheet w/o Matrigel	$0.8–1.5\times10^4$ cells	8–50 weeks	5	none
RNT10	RPE cell sheet w/o Matrigel	$0.8–1.5\times10^4$ cells	26–47 weeks	5	none
RNT9	RPE cell sheet w/o Matrigel	$0.8–1.5\times10^4$ cells	12–38 weeks	5	none

$Log_{10}TPD_{50}$ values for HeLa cells or for hiPSC 201B7 cells following subretinal transplantation to nude rats (upper panel). Subretinal tumorigenicity tests conducted using nude rats under various conditions (lower panel).

doi:10.1371/journal.pone.0085336.t003

space, besides the difference in the status of immunodeficiency in these species or use of Matrigel. We suggest that the environmental effects of the subretinal space are mediated by PEDF secreted by RPE. The close protein sequence identity between human PEDF and the rat counterpart support this idea.

As many as 1×10^4 hiPSC cells were required to form tumors in the subretinal space of nude rats. Similar numbers ($0.8–1.5\times10^4$) of hiPSC-derived RPE were transplanted into the subretinal space in the tumorigenicity test. Note that tumorigenicity testing of iPSC-derived RPE via clinical administration route will always give ''negative'' results, if we aim to detect a tumor from remaining small number of undifferentiated hiPSCs in final product. In this context, tumorigenicity tests conducted by transplanting serial dilutions of hiPSCs combined with hiPSC-derived RPEs into the subretinal space might not be informative. We suggest that tumorigenicity testing via clinical administration route might be useful to detect tumors from intermediate or incompletely differentiated RPE cells, but not for those relatively rare remaining

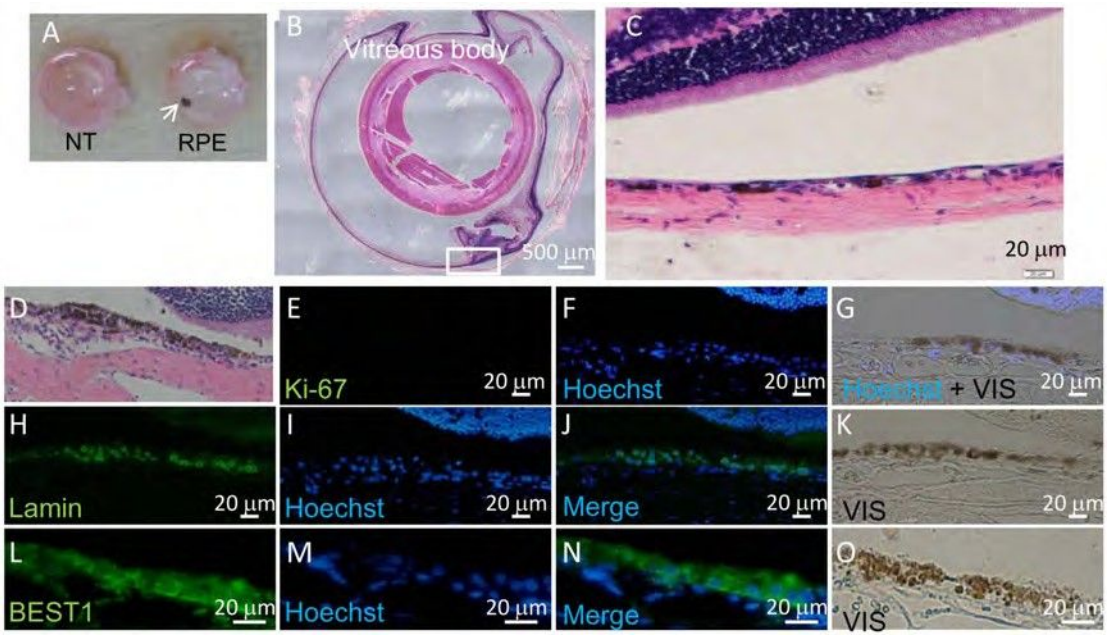

Figure 7. Histological analysis of hiPSC-derived RPE sheets transplanted into the subretinal space of nude rats. (A) Eye balls of nude rat 9 months after subretinal transplantation of $0.8–1.4\times10^4$ hiPSC-derived RPE (in a 1 mm×1 mm cell sheet). Left eye ball transplanted with hiPSC-derived RPE (RPE) and non-transplanted right eye ball (NT). (B) HE staining of cross section of left eye ball following transplantation of hiPSC-derived RPE. (C) HE staining of section of eye ball following transplantation of hiPSC-derived RPE, high magnification. HE- (D), anti-Ki67 antibody- (E), and Hoechst 33258-staining (F) and merged (G) images of serial sections of nude rat retina after transplantation of hiPSC-derived RPE. Anti-Lamin A antibody (H), Hoechst 33258 staining (I), merged (J) and micrographic image (K) of serial sections of nude rat retina after transplantation of hiPSC-derived RPE. Anti-BEST1 antibody (L), Hoechst 33258 (M), merged (N) staining and micrographic image (O) of serial sections of nude rat retina following transplantation of hiPSC-derived RPE.

doi:10.1371/journal.pone.0085336.g007

undifferentiated iPSC. For these reasons, we conducted high dose (1×10^6) subcutaneous RPE transplantation in parallel to examine tumor-forming events from rare hiPSC in hiPSC-derived RPE and full dose hiPSC-derived RPE subretinal transplantation without diluting them with hiPSCs. This was the basis for our rationale in designing multiple tumorigenicity tests for iPSC-derived RPE. As the FDA commentary report[11] stated, the design of tumorigenicity tests should be tailored for each specific product. We hope our approach will facilitate a further discussion related to tumorigenicity testing of iPSC-derived cell products.

Considering the number of rodents used, the duration of the monitoring period, the sensitivity to detect tumors in immunodeficient rodents via both subcutaneous and subretinal administration routes and the overall incidence of tumor formation from iPSC-derived RPE final cell products in these rodents, we conclude that the tumorigenic potential of the hiPSC-derived RPE cells produced by our methods is negligible. Of course, in considering the overall safety of the procedure in humans, discussion should include the site of transplantation as well as the source of the cells (autologous or allogeneic) and the immunesuppression status of the patients.

Materials and Methods

All the experiments using human samples and animal studies were reviewed and approved by the IRB of the Foundation for Biomedical Research and Innovation (FBRI) and Riken Center for Developmental Biology (Riken CDB), and the committee for animal experiments of the FBRI.

Cell Culture

The human iPSC (hiPSC) line 201B7 [12] established from dermal fibroblast with retroviruses pMXs-POU5F1, -Sox2, -c-Myc, and -Klf4 (Riken Bio Resource Center, Tsukuba, Japan) was maintained on feeder layers (SNL [13]) in ReproFF2 (ReproCELL) and 5 ng/mL bFGF (Peprotech). Cell line 836B1 (supplied by CiRA Kyoto University) was established from dermal fibroblast of a healthy donor, and 59, K11, K21, 101, RNT9 or RNT10 lines were derived from dermal fibroblast of 6 patients with retinitis pigmentosa (with a photoreceptor-specific gene mutation) after obtaining informed consent from the patients. These fibroblasts were reprogrammed with episomal EBNA vectors carrying integrated POU5F1, SOX2, KLF4, MYCL, LIN28A and GLIS1 (59-G, K21-G, 101-G, RNT9 and RNT10) or POU5F1, SOX2, KLF4, MYCL, LIN28A and p53shRNA (101-EV, K11-EV and K21-EV). They were established on autologous fibroblast-derived feeders and were maintained in primate ES medium (ReproCELL) with 5 ng/mL bFGF (Wako) [14]. iPSCs were differentiated into retinal pigment epithelium (RPE) as reported previously [15]. iPSC-derived RPE cell clones (59-G3 RPE, K21-G18 RPE, 101-G25 RPE, RNT9 RPE, RNT10 RPE, 101-EV RPE, K11-EV9 RPE or K21-EV15 RPE) were differentiated from the following parental iPSC clones: 59-G3, K21-G18, 101-G25, RNT9-2-8, RNT10-24, 101-EV3, K11-EV9 or K21-EV15, respectively. They were maintained in RPE maintenance medium [5],[15] [DMEM:F12 (7: 3) (Sigma-Aldrich) containing B-27 supplement (Invitrogen), 2 mM L-glutamine (Sigma), 0.5 nM SB431542 (Sigma-Aldrich) and 10 ng/mL bFGF (Wako)]. Human primary RPE (Lonza) was maintained in Retinal Pigment Epithelial Cell Basal Medium (Lonza Biologics, Basel, Switzerland) containing supplements [L-glutamine, GA-1000, and bFGF (Lonza)]. For transplant studies, hiPSC-derived RPE cells in suspension were collected for subcutaneous transplantation or seeded on collagen gel (collagen gel culture kit, Nitta Gelatin) to make a collagen-lined RPE monolayer or double layer cell sheet. The RPE cell sheet was maintained in F10 culture medium (Sigma) and 10% FBS for 4 weeks and RPE maintenance medium for 3 weeks and detached from the collagen gel with collagenase-1 (Roche). The RPE cell sheet was then pipetted and mixed with Matrigel for subcutaneous transplantation or dissected with laser micro dissection (LMD, Carl Zeiss) just before retinal transplantation into animals.

Animal Studies

Mouse subcutaneous transplantation. Various doses of HeLa cells either embedded in 200 mL of Matrigel™ (BD Biosciences) or suspended in 200 mL of PBS (without Matrigel) were injected into subcutaneous tissue of 7- to 8-week-old female nude mice (BALB/cA, JCl-nu/nu; Clea Japan, Inc. Tokyo), SCID mice (C.B-17/Icr-scid/scid, Jcl; Clea), NOD-SCID mice (NOD/ShiJic-scid, Jcl; Clea) or NOG mice (NOD/ShiJic-scid, IL-2R cOD/S KO Jic; Clea) using a 1 mL syringe (TERMO) with a 26 G needle. Animals were monitored for 36 weeks. At the end of the experiments, mice were sacrificed and tumors were removed and fixed with 4% PFA. Paraffin sections were stained with hematoxylin and eosin (HE) for histological observation. Various doses of hiPSC 201B7 cells or 1×10^6 hiPSC-derived RPE cells were embedded in 200 mL of Matrigel™ (BD Bioscience) or suspended in 200 mL of PBS (without Matrigel) and injected subcutaneously into 7- to 8-week-old female NOG mice using a 1 mL syringe (TERMO) with a 26 G needle and monitored for 6–15 months. At the end of the experiments, mice were sacrificed and all the transplants including RPE embedded in 200 mL Matrigel were removed with tweezers and fixed with 4% paraformaldehyde (PFA).

Rat subretinal transplantation. Three-week-old female nude rats (F344/NJcl-rnu/rnu; Clea) were anesthetized by intraperitoneal administration of a mixture of ketamine 100 mg/kg: xylazine 10 mg/kg (Daichi-Sankyo). The pupil of the right eye was dilated with mydriatics (0.5% tropicamide and 0.5% phenylephrine hydrochloride, Santen Pharma). A small incision was made at the right eye corner of the sclera with a 27 G needle. Then, various doses of HeLa cells, hiPSCs or 1 mm×1 mm hiPSC-RPE cell sheets in 2 mL DMEM/F12 medium were injected (Hamilton syringe with 33 G needle) into the subretinal space through the previously made incision in the sclera. The cells or the RPE sheet was transplanted just above the subretinal capillary plexus by observing the position of the Hamilton syringe needle through the dilated pupil under a surgical microscope. The subretinal capillary plexus was readily observed in albino nude rats and was used as a landmark of the subretinal space. The transplanted nude rats were monitored for 8–82 weeks. At the end of the experiments, rats were sacrificed and transplanted whole eye balls were removed and fixed with 4% PFA.

RT-PCR and qRT-PCR

Total RNA was isolated with the RNeasy plus Mini Kit (Qiagen) in accordance with the manufacturer's instructions. Contaminating genomic DNA was removed using a gDNA Eliminator spin column. cDNA was generated from 50 ng of total RNA using PrimeScript RT Master Mix (Takara Bio) and PrimeSTAR MAX DNA Polymerase (TaKaRa Bio). Real-time PCR was then performed with an ABI 7000 Sequence Detection System (Applied-Biosystems) and SYBR-green in accordance with the manufacturer's instruction. Gene expression levels were normalized to that of GAPDH. qRT-PCR was performed using the QuantiTect Probe one-step RT-PCR Kit (Qiagen). The expression levels of target genes were normalized to those of the

RNase P transcript, which were quantified using TaqMan human RNase P control reagents (Applied Biosystems). All qRT-PCR reactions were run for 45 cycles. The sequences of primers and probes used in the present study are listed in Table S1.

Alu PCR

Alu sequences specific to human cells were used to design the primers. The Alu primer 59-AAGTCGCGGCCGCTTGCAGT-GAGCCGAGAT-39 and 50 ng of DNA template, PrimeSTAR Max DNA Polymerase (Takara) were used for PCR reactions (28 cycles). The DNA templates in various ratios (human HeLa DNA: mouse NIH3T3 DNA) were used to determine the human cell detection sensitivity by Alu PCR. PCR products were separated by electrophoresis (MyRun, Cosmobio) with 1% agarose gel (Nacalai), and the image was digitally captured (Bio-Pyramid, Mecan).

Immunohistochemistry

Transplanted tissues were fixed with 4% paraformaldehyde. Paraffin embedded tissue sections were stained with haematoxylin/eosin. Then, the paraffin sections were deparaffinized with xylene and sequential 100%, 95%, 80%, 70% ethanol treatments for 5 min each. The sections were treated with 10 mM citric acid (pH 6) at 95uC for 50 min followed by permeation with 0.4% Triton-X in PBS at room temperature for 30 min. The deparaffinized sections were stained with antibodies against human Lamin-A (1:200; ab108595; Abcam), BEST1 (1:200; ab2182; Abcam) and Ki-67 (1:400; #9449; Cell Signaling). Nuclei were stained with Hoechst 33258 (Dojindo) and DAPI (Dojindo). hiPSC-derived RPE cells were collected in suspension and fixed with 4% paraformaldehyde followed by staining with antibodies against POU5F1 (OCT3/4) (1: 100; sc-5279; Santa Cruz), or BEST1 (1: 200; ab2182; Abcam). Antibodies were visualized with Alexa Fluor 488 goat anti-mouse (1: 1,000; Invitrogen) or Alexa Flour 488 goat anti-rabbit (1: 1,000; Invitrogen). Fluorescent microscopic images were captured with a fluorescent microscope (Olympus BX51, IX71, Tokyo, Japan).

Conclusion

We tested the tumorigenic potential of hiPSC-derived RPE using immuno-deficient rodents. These preclinical tests laid the foundation for upcoming clinical studies using autologous hiPSC-derived RPE sheets for treatment of wet type age-related macular degeneration (AMD). One million hiPSC-derived RPE cells were transplanted subcutaneously into 65 NOG mice and $0.8–1.5\times10^4$ hiPSC-derived RPE cells were transplanted into the subretinal space of 26 nude rats. No tumors were found after 6–15 months of monitoring. Considering the number of rodents used, the duration of the monitoring period, the sensitivity to detect tumors in immuno-deficient rodents, we conclude that the tumorigenic potential of the hiPSC-derived RPE cells prepared by our method is negligible.

Supporting Information

Table S1 Primers for RT-PCR and Alu PCR, Probes and Primers for qRT-PCR are listed.
(DOCX)

Acknowledgments

We thank Yoji Sato of National Institute of Health Sciences, Tokyo for critical reading of the manuscript, Shin-Ichi Nishikawa of JT BRH and Takao Hayakawa of Kinki University for scientific discussions and Mamoru Ito of CIEA for supplying NOG mice.

Author Contributions

Conceived and designed the experiments: H. Kanemura MJG SK. Performed the experiments: H. Kanemura. Analyzed the data: MS NN. Contributed reagents/materials/analysis tools: NS H. Kamao MM CM MT. Wrote the paper: H. Kanemura SK.

References

1. Lu B, Malcuit C, Wang S, Girman S, Francis P, et al. (2009) Long-term safety and function of RPE from human embryonic stem cells in preclinical models of macular degeneration. Stem Cell 27: 2126–2135.
2. Schwartz SD, Hubschman JP, Heilwell G, Franco-Cardenas V, Pan CK, et al. (2012) Embryonic stem cell trials for macular degeneration: a preliminary report. Lancet 379: 713–720.
3. Diniz B, Thomas P, Thomas B, Ribeiro R, Hu Y, et al. (2013) Subretinal implantation of retinal pigment epithelial cells derived from human embryonic stem cells: improved survival when implanted as a monolayer. Invest Ophthalmol Vis Sci. 54: 5087–5096.
4. Hu Y, Liu L, Lu B, Zhu D, Ribeiro R, et al. (2012) A novel approach for subretinal implantation of ultrathin substrates containing stem cell-derived retinal pigment epithelium monolayer. Ophthalmic Res. 48: 186–191.
5. Kuroda T, Yasuda S, Kusakawa S, Hirata N, Kanda Y, et al. (2012) Highly sensitive in vitro methods for detection of residual undifferentiated cells in retinal pigment epithelial cells derived from human iPS cells. PloS One 7: e37342.
6. Müller FJ, Goldmann J, Löser P, Loring JF (2010) A call to standardize teratoma assays used to define human pluripotent cell lines. Cell Stem Cell, 6: 412–414.
7. Prockop DJ (2010) Defining the probability that a cell therapy will produce a malignancy. Mol Ther. 18: 1249–1250.
8. World Health Organization (2010) ''Recommendations for the evaluation of animal cell cultures as substrates for the manufacture of biological medicinal products and for the characterization of cell banks. Proposed replacement of TRS 878, Annex 1.'': ,http://www.who.int/biologicals/BS2132-CS_Recommendations_CLEAN_19_July_2010.pdf..
9. World Health Organization (2008) ''Requirements for the use of animal cells as in vitro substrates for the production of biologicals.WHO Technical Report Series No.878, Annex 1.'': ,http://whglibdoc.who. int/trs/WHO _TRS_878.pdf..
10. Hentze H, Soong PL, Wang ST, Phillips BW, Putti TC, et al. (2009) Teratoma formation by human embryonic stem cells: evaluation of essential parameters for future safety studies. Stem Cell Res. (Amst.) 2: 198–210.
11. Bailey AM (2012) Balancing Tissue and Tumor Formation in Regenerative Medicine. Sci Transl Med. 4: 147fs28.
12. Nakagawa M, Koyanagi M, Tanabe K, Takahashi K, Ichisaka T, et al. (2008) Generation of induced pluripotent stem cells without Myc from mouse and human fibroblasts. Nat. Biotechnol 26: 101–106.
13. Okita K, Ichisaka T, Yamanaka S (2007) Generation of germline-competent induced pluripotent stem cells. Nature 448: 313–317.
14. Maekawa M, Yamaguchi K, Nakamura T, Shibukawa R, Kodanaka I, et al. (2011) Direct reprogramming of somatic cells is promoted by maternal transcription factor Glis1. Nature 474: 225–229.
15. Osakada F, Jin ZB, Hirami Y, Ikeda H, Danjyo T, et al. (2009) In vitro differentiation of retinal cells from human pluripotent stem cells by small-molecule induction. J. Cell. Sci 122: 3169–3179.
16. Quintana E, Shackleton M, Sabel MS, Fullen DR, Johnson TM et al. (2008) Efficient tumour formation by single human melanoma cells. Nature 456: 593–598.
17. Okane H (2009) Strategies toward CNS-regeneration using induced pluripotent stem cells. Genome Informatics 217–220.
18. Ishikawa F, Yasukawa M, Lyons B, Yoshida S, Miyamoto T, et al. (2005) Development of functional human blood and immune systems in NOD/SCID/IL2 receptor gamma chain (null) mice. Blood, 106: 1565–1573.
19. Lewis AM (2005) ''Regulatory Implications of Neoplastic Cell Substrat Tumorigenicity.'': ,http://www.fda.gov/ohrms/dockets/ac/05/slides/5-4188S1_2.ppt..
20. Machida K, Suemizu H, Kawai K, Ishikawa T, Sawada R, et al. (2009) Higher susceptibility of NOG mice to xenotransplanted tumors. J. Toxicol. Sci 34: 123–127.
21. Kanemura H, Go JM, Nishishita N, Sakai N, Kamao H, et al. (2013) Pigment Epithelium-Derived Factor Secreted from Retinal Pigment Epithelium Facilitates Apoptotic Cell Death of iPSC. Scientific Reports 3: 2334.